NPL

Fiducial Reference Measurements for validation of Surface Temperature from Satellites (FRM4STS)
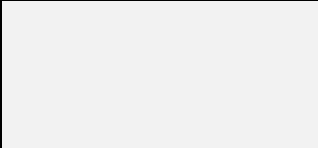
ESA Contract No. 4000113848_15I-LG

D100 - Technical Report 2: Results from the 4th CEOS TIR FRM Field Radiometer Laboratory Inter-comparison Exercise

Part 4 of 4: Land surface temperature comparison of radiation thermometers

JUNE 2017

Reference	OFE-D100(Part 4)-V1-Iss-1-Ver-1-Draft
Issue	1
Revision	1
Date of Issue	22 September 2017
Document Type	TR-2

Approval/Acceptance			
ESA Craig Donlon Technical Officer		**NPL** Andrew Brown Project Manager	Andrew Brown, NPL
	Signature		*Signature*

NPL REPORT ENV 13

2016 comparison of IR brightness temperature measurements in support of satellite validation. Part 4: Land surface temperature comparison of radiation thermometers.

E. Theocharous, I. Barker Snook and N. P. Fox

September 2017

2016 comparison of IR brightness temperature measurements in support of satellite validation. Part 4: Land surface temperature comparison of radiation thermometers.

E. Theocharous, I. Barker-Snook and N. P. Fox
Environmental Division

Abstract

A comparison of terrestrial based infrared (IR) radiometric instrumentation used to support calibration and validation of satellite borne sensors with emphasis on sea/water/land surface temperature was completed at NPL during June and July 2016. The objectives of the 2016 comparison were to establish the "degree of equivalence" between terrestrially based IR Cal/Val measurements made in support of satellite observations of the Earth's surface temperature and to establish their traceability to SI units through the participation of National Metrology Institutes (NMIs). During the 2016 comparison, NPL acted as the pilot laboratory and provided traceability to SI units during laboratory comparisons. Stage 1 consisted of Lab comparisons, and took place at NPL during the week starting on 20th June 2016. This Stage involved laboratory measurements of participants' blackbodies calibrated using the NPL reference transfer radiometer (AMBER) and the PTB infrared radiometer, while participants' radiometers were calibrated using the NPL ammonia heat-pipe reference blackbody. Stage 2 took place at Wraysbury reservoir during the week staring on 27th June 2016 and involved field measurements of the temperature of the surface of the water. Stage 2 included the testing of the same radiometers alongside each other, completing direct daytime and night-time measurements of the surface temperature of the water. Stage 3 took place in the gardens of NPL during the week starting on 4th July 2016 and involved field measurements of the temperature of the surface of a number of solid targets. Stage 3 included the testing of the same radiometers alongside each other, completing direct daytime and night-time measurements of the surface temperature of targets, including short grass, clover, soil, sand, gravel and tarmac/asphalt. This report provides the results of Stage 3, together with uncertainties as provided by the participants, for the comparison of the participants' radiometers. During the 2016 comparison, all participants were encouraged to develop uncertainty budgets for all measurements they reported. All measurements reported by the participants, along with their associated uncertainties, were analysed by the pilot laboratory and are presented in this report.

National Physical Laboratory
Hampton Road, Teddington, Middlesex, TW11 0LW

Approved on behalf of NPLML by Teresa Goodman, Earth Observation, Climate and Optical Group

CONTENTS

1. INTRODUCTION

The measurement of the Earth's surface temperature and, more fundamentally, its temporal and spatial variation, is a critical operational product for meteorology and an essential parameter for climate monitoring. Satellites have been monitoring global surface temperature for some time. However, it is essential for long-term records that such measurements are fully anchored to SI units.

Field-deployed infrared radiometers (see footnote 1) currently provide the most accurate surface-based measurements which can be used for calibration and validation of satellite/airborne Earth observation radiometers. These radiometers are in principle calibrated traceably to SI units, generally through a blackbody radiator. However, they are of varying design and are operated by different teams in different parts of the globe. It is essential for the integrity of their use, that any differences in their measurements are understood, so that any potential biases are removed and are not transferred to satellite sensors.

Under the auspices of the Committee on Earth Observation Satellites (CEOS) a comparison of terrestrial based infrared (IR) radiometric instrumentation used to support calibration and validation of satellite borne sensors with emphasis on sea/water surface temperature was completed in Miami in 2001 (Barton et al., 2004) (Rice et al., 2004) and at NPL and Miami in 2009 (Theocharous et al. 2010), (Theocharous and Fox, 2010). However, seven years had passed, and as many of the satellite sensors originally supported were nearing the end of their life, a similar CEOS comparison was repeated in 2016 through an ESA funded project called FRM4STS (www.FRM4STS.org). The objectives of the 2016 comparison were to establish the "degree of equivalence" between terrestrially based IR Cal/Val measurements made in support of satellite observations of the Earth's surface temperature and to rigorously establish their traceability to SI units through the participation of NMIs.

2. ORGANISATION OF THE COMPARISON

During the 2016 comparison, NPL acted as the pilot laboratory and, with the aid of PTB, provided traceability to SI units during laboratory comparisons. The logistics and planning of the comparisons was led by NPL with support from PTB, University of Southampton, RAL, KIT, DMI and ESA. The 2016 comparison consisted of three stages. Stage 1 took place at NPL in June 2016 and involved laboratory measurements of participants' blackbodies calibrated using the NPL reference transfer radiometer (AMBER) (Theocharous et al., 1998) and the PTB infrared radiometer, while the performance of the participants' radiometers was compared using the NPL ammonia heat-pipe reference blackbody. The performance of 8 blackbodies and 19 radiometers operating at a range of different measurement wavelength channels in the thermal infrared part of the spectrum was compared during Stage 1. Stage 2 took place on a floating platform located in the middle of Wraysbury reservoir in June/July 2016. The performance of 10 radiometers was compared during Stage 2. Stage 2 included the testing of the participating radiometers alongside each other, completing direct daytime and night-time measurements of the skin temperature of the reservoir water. Stage 3 took place in the gardens of NPL during the week starting on 4th July 2016 and involved field measurements of the temperature of the

---

1 This report describes the comparison of instruments which are referred to by participants as "radiometers". However, radiometers generally measure and report radiometric parameters in radiometric units (W, Wm^{-2}, etc.). The instruments dealt with here measure temperature (in units of degrees C or K) so formally they are thermometers or "radiation thermometers". However, in view of the common usage of the terminology for this application, this report will continue to use the term "radiometer".

surface of a number of solid targets. Stage 3 included the testing of the same radiometers alongside each other, completing direct daytime and night-time measurements of the surface temperature of targets, including short grass, clover, soil, sand, gravel and tarmac/asphalt.

This report provides the results, together with uncertainties as provided by the participants, of the measurement of the Land Surface Temperature (LST) of six solid surfaces as representatives of differing texture, emissivity and thermal complexity. The laboratory comparison of the participants' blackbodies, as measured by the NPL AMBER radiometer and the PTB infrared radiometer and the lab radiometer comparison as well as the WST comparison at Wraysbury reservoir are presented in other reports (Barker Snook et al., 2017), (Barker Snook et al., 2017a), Theocharous et al., 2017).

The 2016 LST radiometer comparison at NPL consisted of mounting the participating radiometers on a specially erected steel frame so they could view the sample which was placed at the base of this frame. Figure 1 shows the steel frame on which the radiometers were mounted during the comparison of the surface temperature of the sand sample. The participating radiometers had different Fields of View (FoV) so they were mounted on the steel frame at different heights from the ground so that the area of the sample being viewed by the radiometers was approximately the same (for further discussion on this, see Section 5.1). Three of the samples (the short grass, clover and the asphalt/tarmac sample) monitored during the 2016 comparison occurred naturally in the NPL gardens whereas the remaining three (sand, soil and gravel) were specially set up by building wooden frames and filling them with samples purchased from a local store. Photos of the six samples used during the 2016 LST comparison at NPL can be seen in Appendix 1 of this report. The frame on which the radiometers were mounted was moved to the place where the appropriate sample was located, following a procedure agreed by all participants.

During the majority of the duration of the 2016 LST comparison at NPL, changing weather conditions prevailed. This was not ideal for the LST radiometer comparison but participants persevered with their measurements none the less, due to the tight time schedule.

Figure 1: Radiometers mounted on the steel frame during the comparison of the surface temperature of the sand sample contained in the wooden frame.

3. PARTICIPANTS' RADIOMETERS AND MEASUREMENTS

Section 3 gives brief descriptions of the radiometers participating in the LST comparison at NPL together with the measurements which were completed by the radiometers during these comparisons, along with the associated combined uncertainty values which were provided by the participants. Section 3 also provides the uncertainty budgets of the measurements completed using the participating radiometers, as provided by the participants. In some cases the level of detail provided by participants in the uncertainty budgets of their measurements is fairly limited and not ideal. However, whatever was provided by the participants is included in this report, along with a summary of the results for each participant for each stage of the comparison.

3.1 LST MEASUREMENTS PROVIDED BY VALENCIA UNIVERSITY

Dept. of Earth Physics and Thermodynamics, University of Valencia.
50, Dr. Moliner. ES-46100, Burjassot (Valencia), Spain
Contact Names: César Coll and Raquel Niclòs
Email: cesar.coll@uv.es , raquel.niclos@uv.es

3.1.1   Description of the Radiometer and Route of Traceability
Type of Radiometer: CIMEL Electronique CE312-2, six spectral bands (unit 2)

Technical description of the radiometer

Type of detector: thermopile, operating at ambient temperature.
Six spectral bands: B1 (8.0-13.3 μm), B2 (10.9-11.7 μm), B3 (10.2-11.0 μm), B4 (9.0-9.3 μm), B5 (8.5-8.9 μm), and B6 (8.3-8.6 μm).
Broad band: Germanium window and zinc sulphide filters determined spectral responsivity.
Narrow bands: Interference filters determined spectral responsivity.
Field of view of radiometer: 10º.

The instrument has a built-in radiance reference made of a concealable gold-coated mirror which enables comparison between the target radiance and the reference radiation from inside the detector cavity. The temperature of the detector is measured with a calibrated Platinum Resistance Thermometer (PRT), thus allowing compensation for the cavity radiation. The relevant outputs of the radiometer are the detector temperature and the difference in digital counts between the signals from the target and the detector cavity.

Establishment or traceability route for primary calibration including date of last realisation and breakdown of uncertainty

Band 2 (10.9-11.7 μm) of CE-312-2 (unit 2) was used for retrieving LST from the brightness temperature measurements at NPL because land surface emissivities are usually higher at this band. The following uncertainty analysis is based on laboratory measurements with the Landcal blackbody P80P. The total uncertainty of this blackbody was 0.34 K (Theocharous et al 2017, Barker-Snook et al. 2017), see also estimates from Sicard et al. (1999) and Legrand et al. (2000). Blackbody measurements were taken at six fixed temperatures in the 0 to 50 ºC temperature range in two different runs with instrument realigning. The values reported below are typical values for all blackbody temperatures considered for band 2 of unit 2.

Type A

- Repeatability: 0.03 K, 0.012% (at 300 K). Typical value of the standard deviation of 15 measurements at fixed black body temperature without re-alignment of radiometer.

- Reproducibility: 0.06 K, 0.018% (at 300 K).Typical value of difference between two runs of radiometer measurements at the same blackbody temperature including re-alignment.

Total Type A uncertainty (RSS): 0.07 K, 0.022% (at 300 K).

Type B

- Primary calibration: 0.34 K (estimation of the total uncertainty of the Landcal blackbody P80P).

- Land surface emissivity: Emissivity values for the different targets of the comparison (sand, soil, gravel, clover and tarmac) were obtained using the Temperature and Emissivity Separation (TES) method (Gillespie et al., 1998), which requires multiband measurements of surface-leaving and downwelling sky radiances and provides simultaneous retrieval of band emissivities and LST. It is based on an empirical relationship between the apparent spectral contrast in band emissivities (or maximum-minimum emissivity difference, MMD) and the minimum band emissivity. The resulting emissivity values and uncertainties for band 2 were:

Sand:	0.963 ± 0.010
Soil:	0.976 ± 0.013
Gravel:	0.966 ± 0.010
Clover:	0.978 ± 0.011
Tarmac:	0.973 ± 0.010

Data were available for the gravel target on two days (July 6 and 7), the resulting band 2 emissivity being identical in both cases (0.966 ± 0.010). The downwelling sky radiance was measured near-simultaneously to the surface radiance using a diffuse reflectance gold panel. During the measurement campaign, atmospheric conditions were not ideal, with cloud cover changing very quickly during the measurements. Therefore, sky radiance was rather variable showing sky temperatures ranging from -7 to -27 ºC, which is roughly equivalent to a variation of ±15 % in downwelling sky radiance (band 2). Using the above uncertainty estimates, the emissivity values and typical LST and sky temperatures for each surface, the uncertainty obtained for the emissivity and sky radiance correction of brightness temperatures is:

Sand:	0.45 K
Soil:	0.55 K
Gravel:	0.49 K
Clover:	0.35 K
Tarmac:	0.52 K

- Angle of view to nadir: 0.02 K. An uncertainty of 2.5° in zenith angle was considered for the analysis, which results in emissivity uncertainty of 0.0003 at an observation angle of 25º from nadir (García-Santos et al., 2012).

- Linearity of radiometer: 0.06 K. Typical value for all bands in the temperature range 0-40 ºC according to Legrand et al. (2000).

- Drift since calibration: It has been corrected for using the calibration measurements performed with the Landcal blackbody P80P mentioned above. A linear correcting equation has been derived for each band and radiometer, with the radiometer measured temperature and the detector temperature as inputs. The uncertainty for this correction is the RSS of the typical estimation uncertainty of the linear regression (0.04 K for unit 2) and the uncertainties resulting from the propagation of input temperature errors (standard deviations for 15 measurements at a fixed temperature) in the linear correcting equation. The resulting uncertainty in the correction of calibration drift is 0.05 K for unit 2.

- Ambient temperature fluctuations: The effect of ambient temperature fluctuations is compensated by the CE-312 radiometers by measuring the detector cavity temperature by means of a calibrated PRT. The uncertainty in this process is the uncertainty of the internal PRT, which is 0.04 K according to Legrand et al. (2000).

- Atmospheric absorption/emission: 0.02 K. The vertical distance between the radiometer was taken as 2.5 m and the surface and observation angle from nadir as 25º. Atmospheric transmittances and upwelling radiances were simulated with the MODTRAN 5 radiative model and NCEP atmospheric profiles suitable for the campaign conditions.

Total Type B uncertainty (RSS):
Sand: 0.57 K
Soil: 0.65 K
Gravel: 0.60 K
Clover: 0.50 K
Tarmac: 0.63 K

Type A + Type B uncertainty (RSS):
Sand: 0.58 K
Soil: 0.66 K
Gravel: 0.61 K
Clover: 0.50 K
Tarmac: 0.63 K

References:

García-Santos, V., E. Valor, V. Caselles, M. Á. Burgos and C. Coll (2012). On the angular variation of thermal infrared emissivity of inorganic soils, Journal of Geophysical Research, Vol. 117, D19116, doi:10.1029/2012JD017931, 2012

Gillespie, A. R., T. Matsunaga, S. Rokugawa, and S. J. Hook (1998). Temperature and emissivity separation from Advanced Spaceborne Thermal Emission and Reflection Radiometer (ASTER) images, IEEE Transactions on Geoscience and Remote Sensing, 36, 1113-1125.

Legrand, M., C. Pietras, G. Brogniez, M. Haeffelin, N. K. Abuhassan and M. Sicard (2000). A high-accuracy multiwavelength radiometer for in situ measurements in the thermal infrared. Part I: characterization of the instrument, J. *Atmos. Ocean Techn., 17*, 1203-1214.

Sicard, M., Spyak, P. R., Brogniez, G., Legrand, M., Abuhassan, N. K., Pietras, C., and Buis, J. P. (1999). Thermal infrared field radiometer for vicarious cross-calibration: characterization and comparisons with other field instruments. *Optical Engineering*, 38 (2), 345-356.

Operational methodology during measurement campaign:
Unit 2 of the CE-312-2 radiometer was used for surface radiance measurements; however, we had problems with data transmission from the radiometer to the data-logger on July 4 and 5 resulting in no data available on those days. We were able to collect data on July 6 (golden day: sand, soil, gravel, clover and tarmac) and 7 (gravel). For these measurements, the radiometer was mounted on the frame next to the other participant radiometers and all were aligned to observe approximately the same area on the target. This was repeated every time the target was

changed. We planned to use unit 1 of radiometer CE-312-2 for continuous measurements of downwelling sky radiance simultaneously to the surface measurements of unit 2. However, unit 1 showed electronic and power problems during the campaign and did not provide useful data. Therefore, sky radiance measurements were performed with unit 2 by placing the diffuse reflectance gold panel in the field of view of the radiometer at regular, short intervals during the measurement of surface radiances. The measured sky radiances were then interpolated to the time of the surface radiance measurements.

3.1.2 Uncertainty Contributions Associated with LST Measurements made by Valencia University at NPL

The tables below show the uncertainty breakdown for the measurement of LST at NPL. The RMS total refers to the square root of the sum of the squares of all the individual uncertainty terms. One table is given for each of the surface targets measured (sand, soil, gravel, clover and tarmac).

SAND

Uncertainty Contribution	Type A	Type B	
	Uncertainty in Value / %	Uncertainty in Value / (appropriate units)	Uncertainty in temperature (K)
Repeatability of measurement	0.012		0.03
Reproducibility of measurement	0.018		0.06
Primary calibration		0.34 K	0.34
Land target emissivity		0.010 in emissivity, 15% in downwelling irradiance	0.45
Angle of view to nadir		2.5° in viewing angle	0.02
Linearity of radiometer			0.06
Drift since calibration			0.05
Ambient temperature fluctuations			0.04
Atmospheric absorption/emission			0.02
RMS total	0.07 K / 0.022 %	0.57 K	0.58

SOIL

Uncertainty Contribution	Type A	Type B	
	Uncertainty in Value / %	Uncertainty in Value / (appropriate units)	Uncertainty in temperature (K)
Repeatability of measurement	0.012		0.03
Reproducibility of measurement	0.018		0.06
Primary calibration		0.34 K	0.34
Land target emissivity		0.013 in emissivity, 15% in downwelling irradiance	0.55
Angle of view to nadir		2.5° in vieving angle	0.02
Linearity of radiometer			0.06
Drift since calibration			0.05
Ambient temperature fluctuations			0.04
Atmospheric absorption/emission			0.02
RMS total	0.07 K / 0.022 %	0.65 K	0.66

GRAVEL

Uncertainty Contribution	Type A	Type B	
	Uncertainty in Value / %	Uncertainty in Value / (appropriate units)	Uncertainty in temperature (K)
Repeatability of measurement	0.012		0.03
Reproducibility of measurement	0.018		0.06
Primary calibration		0.34 K	0.34
Land target emissivity		0.010 in emissivity, 15% in downwelling irradiance	0.49
Angle of view to nadir		2.5° in vieving angle	0.02
Linearity of radiometer			0.06
Drift since calibration			0.05
Ambient temperature fluctuations			0.04
Atmospheric absorption/emission			0.02
RMS total	0.07 K / 0.022 %	0.60 K	0.61

CLOVER

Uncertainty Contribution	Type A	Type B	
	Uncertainty in Value / %	Uncertainty in Value / (appropriate units)	Uncertainty in temperature (K)
Repeatability of measurement	0.012		0.03
Reproducibility of measurement	0.018		0.06
Primary calibration		0.34 K	0.34
Land target emissivity		0.011 in emissivity, 15% in downwelling irradiance	0.35
Angle of view to nadir		2.5° in vieving angle	0.02
Linearity of radiometer			0.06
Drift since calibration			0.05
Ambient temperature fluctuations			0.04
Atmospheric absorption/emission			0.02
RMS total	0.07 K / 0.022 %	0.50 K	0.50

TARMAC

Uncertainty Contribution	Type A	Type B	
	Uncertainty in Value / %	Uncertainty in Value / (appropriate units)	Uncertainty in temperature (K)
Repeatability of measurement	0.012		0.03
Reproducibility of measurement	0.018		0.06
Primary calibration		0.34 K	0.34
Land target emissivity		0.010 in emissivity, 15% in downwelling irradiance	0.52
Angle of view to nadir		2.5° in vieving angle	0.02
Linearity of radiometer			0.06
Drift since calibration			0.05
Ambient temperature fluctuations			0.04
Atmospheric absorption/emission			0.02
RMS total	0.07 K / 0.022 %	0.63 K	0.63

3.1.3 LST Measurements provided by Valencia University

Figures 2, 3, 4a and 4b show the measurements completed by the Valencia University radiometer on clover, gravel, soil and sand respectively. The uncertainty bars shown in the figures represent the uncertainty values provided by Valencia University which correspond to the measurements shown in the Figures.
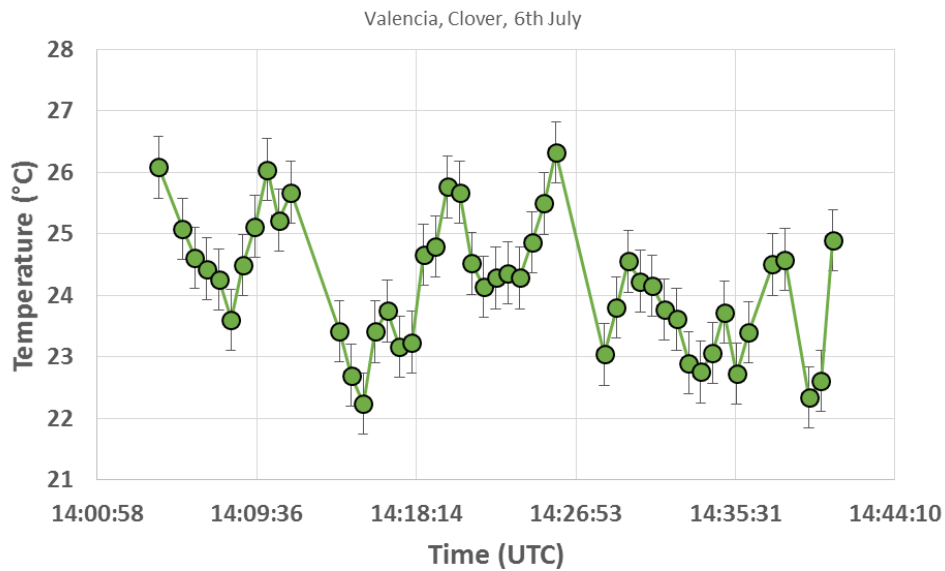
Figure 2: Surface temperature of clover measured by Valencia University on the 6th July 2016
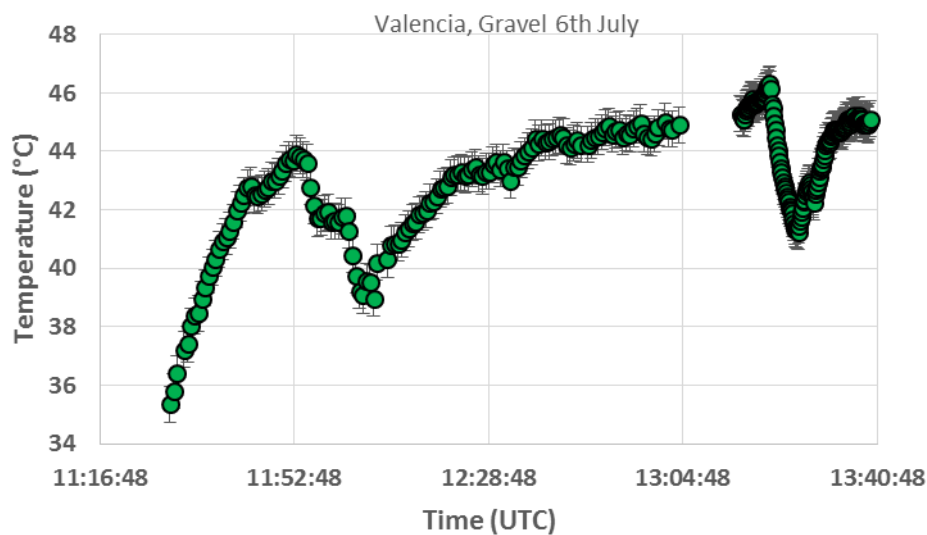
Figure 3: Surface temperature of gravel measured by Valencia University on the 6th July 2016
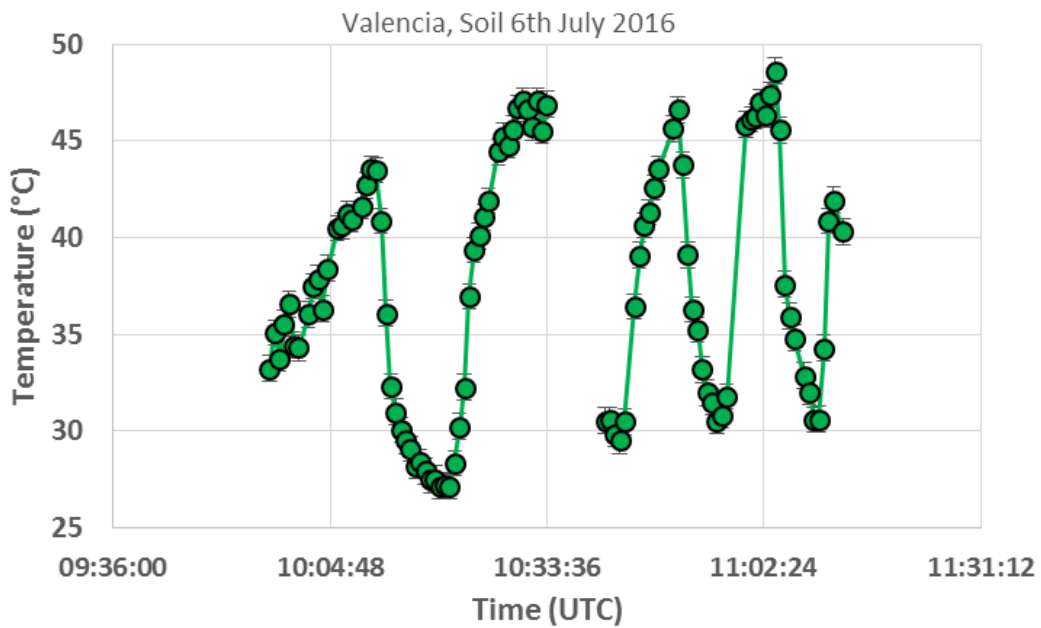
Figure 4a: Surface temperature of soil measured by Valencia University on the 6th July 2016
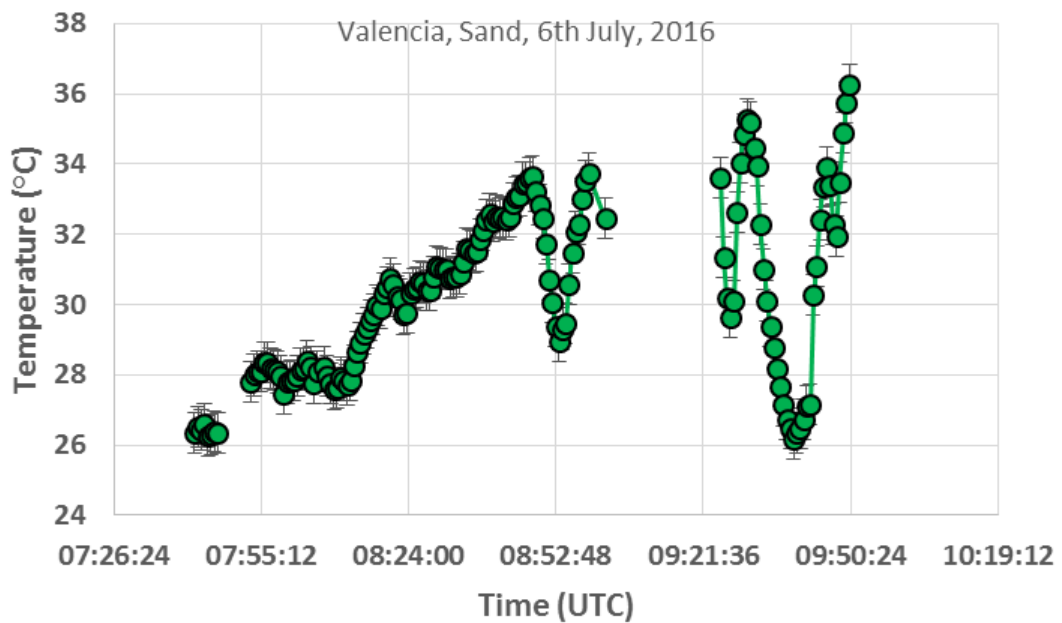
Figure 4b: Surface temperature of sand measured by Valencia University on the 6th July 2016

3.2   LST Measurements provided by JPL

NASA/Jet Propulsion Laboratory
California Institute of Technology
Contact Name: Gerardo Rivera
e-mail: gerardo.rivera@jpl.nasa.gov

3.2.1   Descrption of the JPL radiometer

Information on the JPL participating radiometer can be found
on: http://calval.jpl.nasa.gov/radiometers.

The JPL participating Radiometer is based on the Apogee SI-121 radiometer. The Apogee SI-121 Radiometer is considered a narrow field-of-view infrared radiometer sensor with an 18 degree half-angle and a response time of 0.6 seconds.

The Measurement Repeatability of the JPL radiometer is less than 0.05 °C.
The Stability (Long-term Drift) of the JPL radiometer is less than 2 % change in slope per year when the germanium filter is maintained in a clean condition.
The Response Time (defined as the time for detector signal to reach 95 % following a step change of the input of the JPL radiometer) is 0.6 s.
The Spectral Range of the radiometer extends over the 8 μm to 14 μm atmospheric window
The Operating Environment of the radiometer is from -55 °C to 80 °C, over the 0 to 100 % relative humidity range.

3.2.2   Uncertainty of the JPL radiometer

Ali Abtahi of JPL has clarified the uncertainty of the JPL Radiometers.   The uncertainty of the JPL radiometer is based on the uncertainty of the Apogee SI-121 radiometer (on which the JPL radiometer is based) but the uncertainty also depends on the Platinum thermoelectric modules which are also used within the JPL radiometer.

The uncertainty value which should be used with the JPL radiometer is 0.1 °C when measurements in the temperature range -10 °C to +60 °C are being made in ambient temperature environments of +4 °C to +44 °C.

3.2.3   LST Measurements provided by JPL

Figures 5, 6, 7, 8, 9 and 10 show the measurements completed by the JPL radiometer on clover, short grass, gravel, sand, soil and tarmac/asphalt, respectively. The uncertainty bars in the figures represent the uncertainty values provided by JPL which correspond to the measurements shown in the Figures.
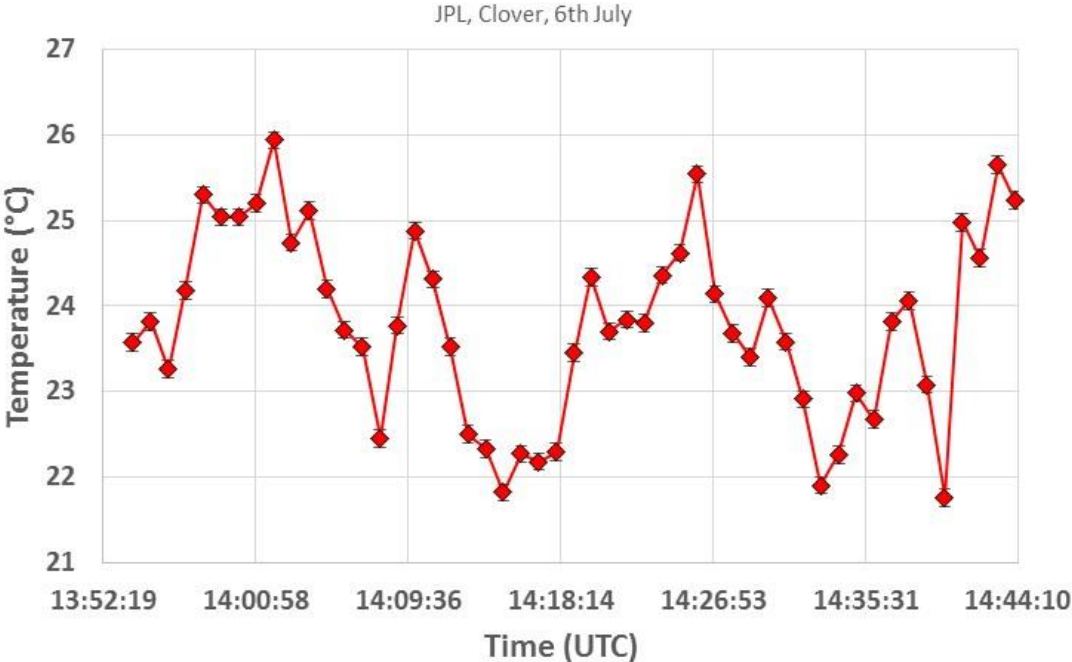
Figure 5: Surface temperature of clover measured by JPL on the 6th July
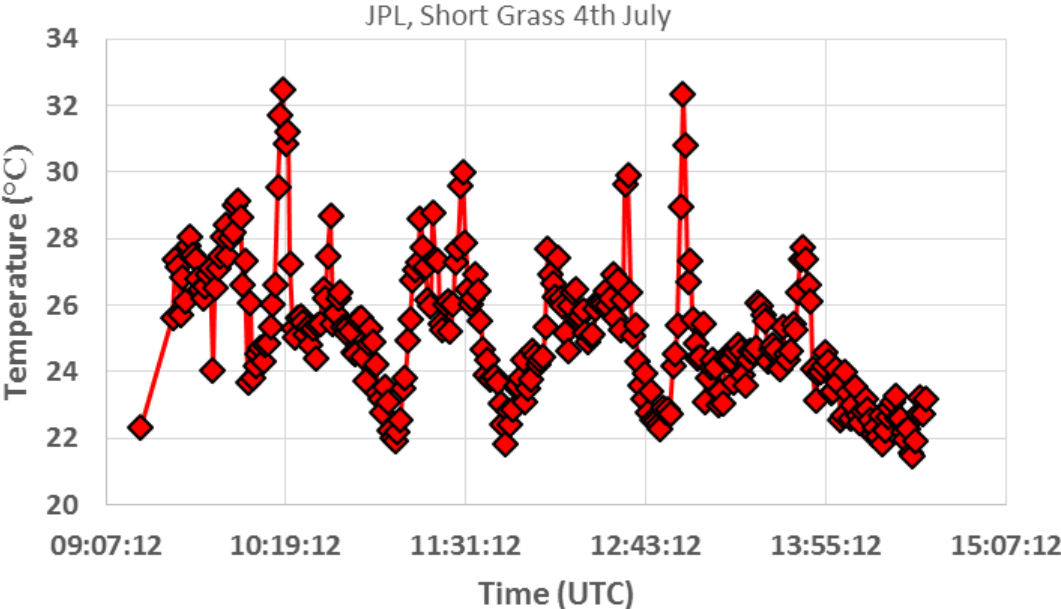

Figure 6: Surface temperature of short grass measured by JPL on the 4th July
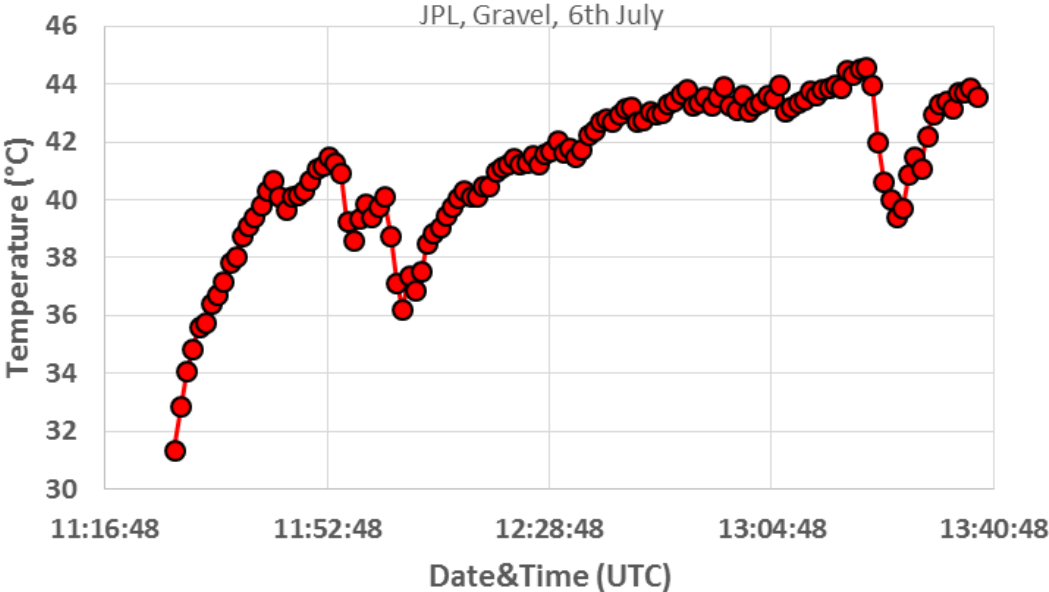
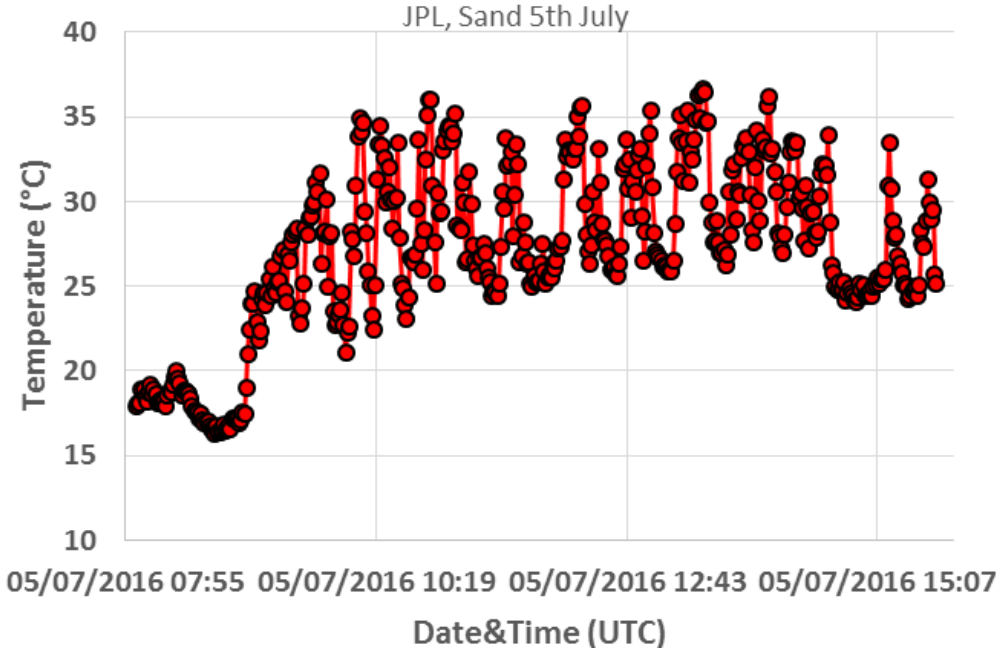Figure 7: Surface temperature of gravel measured by JPL on the 6th July

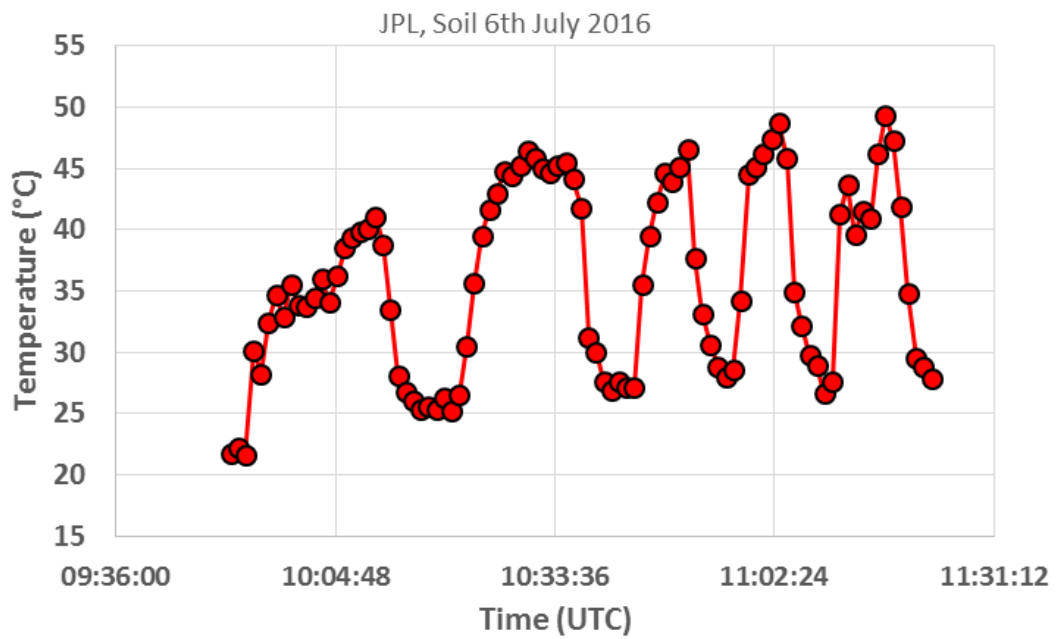Figure 8: Surface temperature of sand measured by JPL on the 5th July

Figure 9: Surface temperature of soil measured by JPL on the 6th July
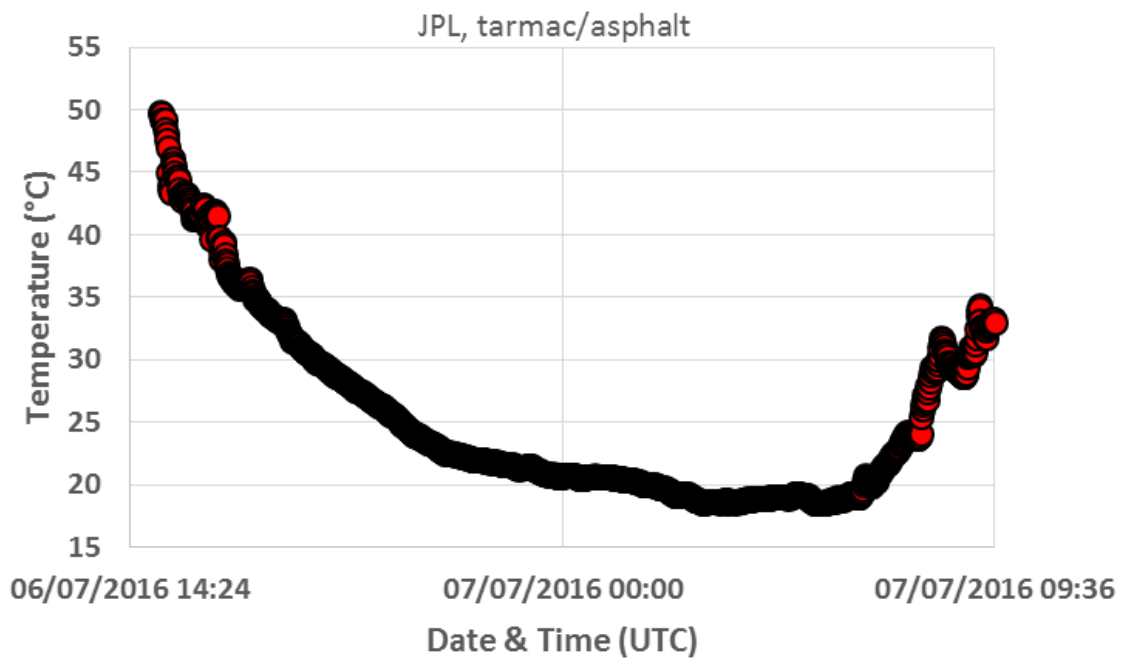

Figure 10: Surface temperature of tarmac measured by JPL on the 6th and 7th July

3.3 LST MEASUREMENTS PROVIDED BY KIT

IMK-ASF, Karlsruhe Institute of Technology (KIT)
Hermann-von-Helmholtz-Platz 1, 76344 Eggenstein-Leopoldshafen, Germany
Contact Name: Dr. Frank-M. Goettsche.
e-mail: frank.goettsche@kit.edu

Description of KIT's Radiometer and route of traceability

Make and type of Radiometer: Heitronics KT15.85 IIP with L6 lens

Outline Technical description of instrument: The KT15.85 IIP is a single channel radiometer based on a pyroelectric infrared detector. This type of sensor links radiance measurements via beam-chopping to internal reference temperature measurements and thermal drift can practically be eliminated. The KT15.85 IIP covers the spectral range from 9.6 µm to 11.5 µm, has an uncertainty of about 0.3 K over the temperature range relevant to land surfaces and offers excellent long-term stability. The response time of the surface observing radiometer (serial #11650) was set to 10 sec and its temperature range to -25 °C to +100 °C. The type L6 lens used has a full-view angle of 8.3° and is well-suited for directional measurements.

Establishment of traceability route for primary calibration including date of last realisation and breakdown of uncertainty:
Primary calibrations to within specifications were performed on the 03.07.2015 (serial #11650) and 05.05.2015 (serial #11615) by Heitronics GmbH, Wiesbaden, Germany. Breakdowns of uncertainties are not available.

Operational methodology during measurement campaign:

Radiometers were aligned using a Heitronics target laser designed for the KT15.85 IIP.

The LST experiments at NPL were performed over small, artificial targets; no sampling strategy was applied. The representativeness of the KT15.85 IIP 'ground' measurements was increased by raising it 4 m above the ground: together with a view angle of about 20° this yielded a FOV of about 60 cm in diameter. The second KT15.85 IIP radiometer (serial #11615, temperature range -100 °C to +100 °C) was deployed for simultaneously obtaining down-welling 'sky' radiance. Measurements were taken every 10 sec by a Campbell Scientific CR1000 data logger and averaged over 1 minute.

With the exception of the grass and clover targets (for which emissivities were obtained from literature), emissivities were obtained from single-lid emissivity box (Rubio et al., 1997) measurements with the KT15.85 IIP (spectral range 9.6 µm - 11.5 µm):

Sand:	0.952 ± 0.010
Garden Soil (dark):	0.982 ± 0.007
Tarmac:	0.959 ± 0.005
Pebbles (gravel):	0.959 ± 0.003
Grass(semi-dry, short):	0.980 ± 0.010
Clover:	0.985 ± 0.005

The data processing and the emissivity box methods are described in:

Göttsche, F.-M., Olesen, F.-S., Trigo, I., Bork-Unkelbach, A., and Martin, M. (2016). Long Term Validation of Land Surface Temperature Retrieved from MSG/SEVIRI with Continuous in-Situ Measurements in Africa. *Remote Sensing*, MDPI AG, Vol. 8, 410, doi:10.3390/rs8050410

Göttsche, F.-M., and Hulley, G. C. (2010). Validation of six satellite-retrieved land surface emissivity products over two land cover types in a hyper-arid region. *Remote Sensing of Environment*, Vol. 124, pp. 149-158, doi:10.1016/j.rse.2012.05.010

Rubio, E., Caselles, V., and Badenas, C. (1997). Emissivity Measurements of Several Soils and Vegetation Types in the 8-14 micrometer Wave Band: Analysis of Two Field Methods. *Remote Sensing of Environment*, Vol. 59, pp. 490-521

Radiometer usage (deployment), previous use of instrument and planned applications.

The KT15.85 IIP's were used for inter-calibrations at KIT's validation stations Dahra, Senegal and Evora, Portugal. They will be deployed for several years in support of KITs long-term satellite LST validation activities.

3.3.2   LST: Uncertainty Contributions associated KIT's measurements at NPL

Table 3.3.1 shows the uncertainty contributions associated KIT's LST measurements at NPL.

The reported uncertainty is based on a standard uncertainty (coverage factor k=1), providing a confidence level of approximately 68%.

Comments:
Estimates are given for a representative emissivity of 0.970 and assume 20 K temperature difference between target and sensor housing. Relative uncertainties are 'at reading' at 25 °C.

Comment: Uncertainty due to spatial temperature variations in the radiometer's FOV has not been specified. Measuring over homogeneous surfaces and / or ensuring sufficiently large FOVs (e.g. by raising the radiometer) can make spatial temperature variations negligible; this was the approach taken in the LST experiments. A detailed analysis of LST uncertainty is given in: Göttsche, Frank-M., Olesen, Folke-S., Trigo, Isabel F., Bork-Unkelbach, Annika, and Martin, Maria A. (2016), "Long Term Validation of Land Surface Temperature Retrieved from MSG/SEVIRI with Continuous in-Situ Measurements in Africa", *Remote Sensing*, **8**, 410, doi:10.3390/rs8050410

Table 3.3.1: Uncertainty Contributions associated KIT's measurements at NPL

Uncertainty Contribution	Type A Uncertainty in Value / %	Type B Uncertainty in Value / (appropriate units)	Uncertainty in Brightness temperature K
Repeatability of measurement	0.57		0.143
Reproducibility of measurement	0.57		0.143
Primary calibration		0.250 K	0.250
Target emissivity		0.5 %	0.333
Linearity of radiometer		0.070 K	0.070
Drift since calibration		0.179 K	0.179
Resolution of radiometer		0.035 K	0.035
Ambient temperature fluctuations		0.035 K	0.035
Atmospheric absorption/emission		0.035 K	0.035
Down-welling sky radiance		0.011 K	0.011
RMS total	0.81 %		0.505 K

3.3.3 LST Measurements completed by KIT

Figures 11, 12, 13, 14, 15 and 16 show the measurements completed by the KIT radiometer on clover, short grass, gravel, sand, soil and tarmac/asphalt, respectively. The uncertainty bars in the figures represent the uncertainty values provided by KIT which correspond to the measurements shown in the Figures.
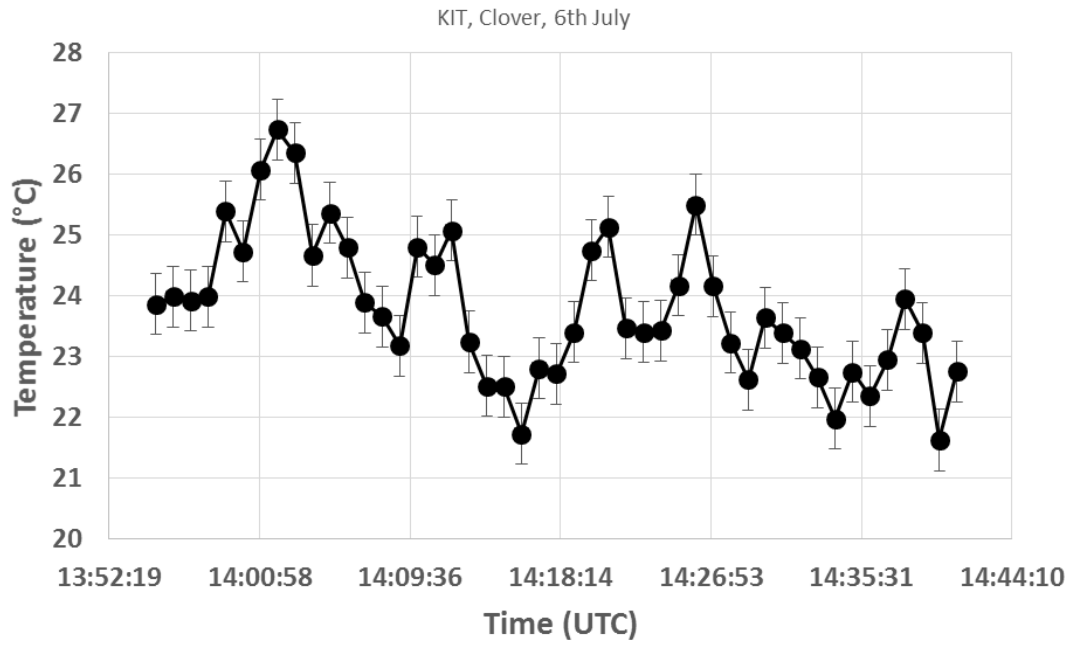
Figure 11: Surface temperature of clover measured by KIT on the 6th July
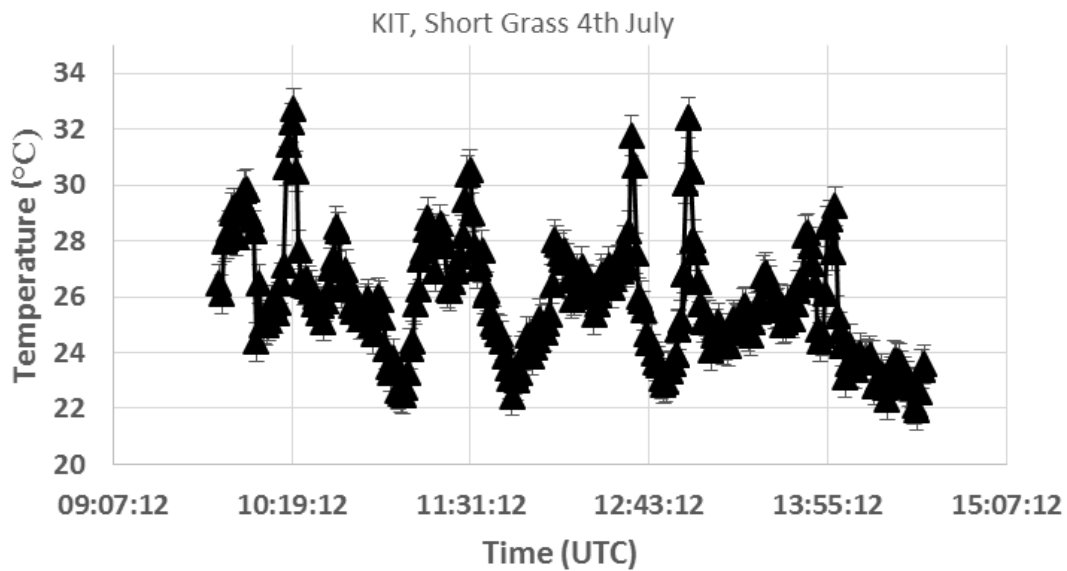
Figure 12: Surface temperature of short grass measured by KIT on the 4th July
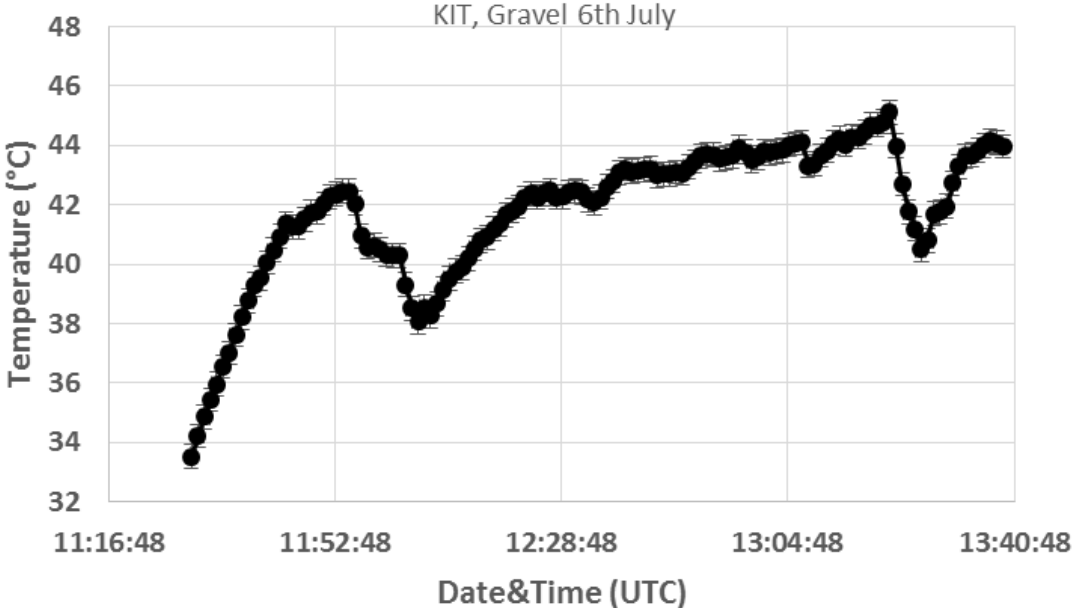
Figure 13: Surface temperature of gravel measured by KIT on the 6th July
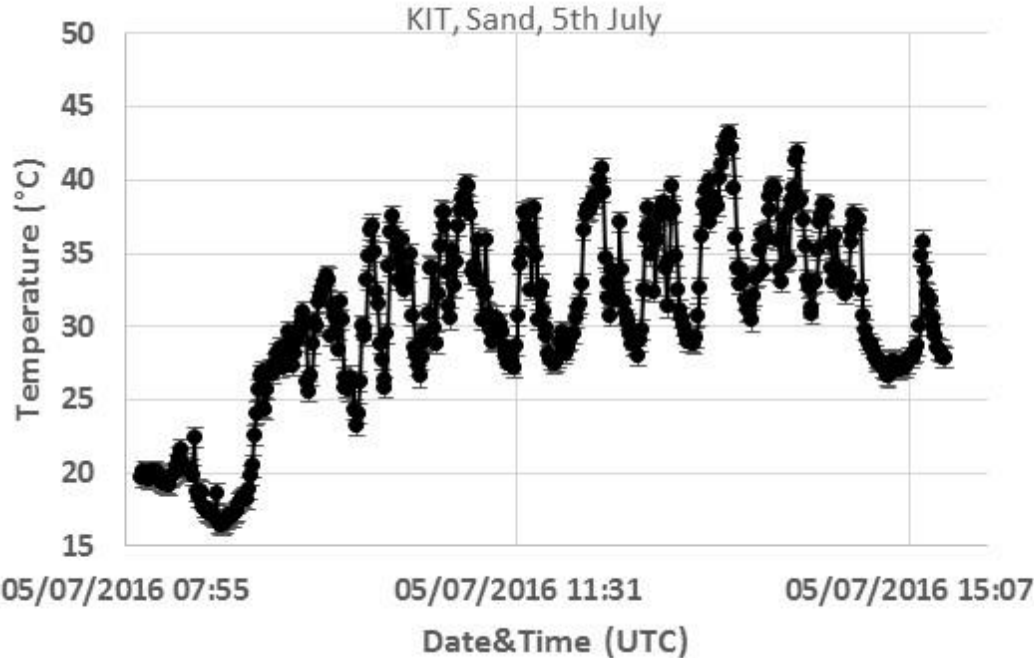
Figure 14: Surface temperature of sand measured by KIT on the 5th July
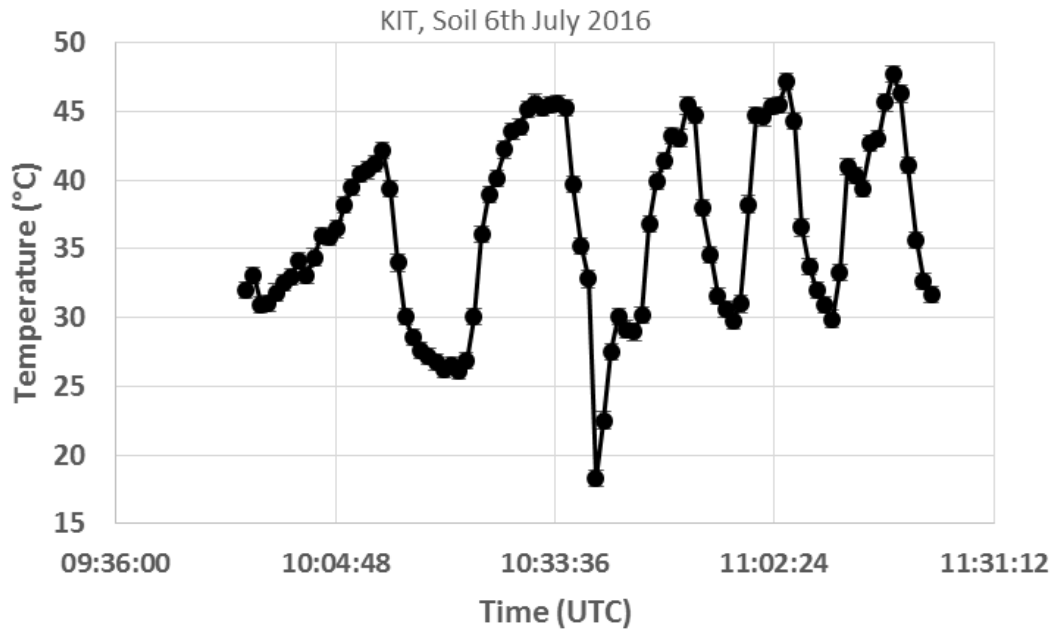
Figure 15: Surface temperature of soil measured by KIT on the 6th July. The spike which appears at about 10:39 AM arose due to the partial obscuration of the radiometer FoV by a participant.
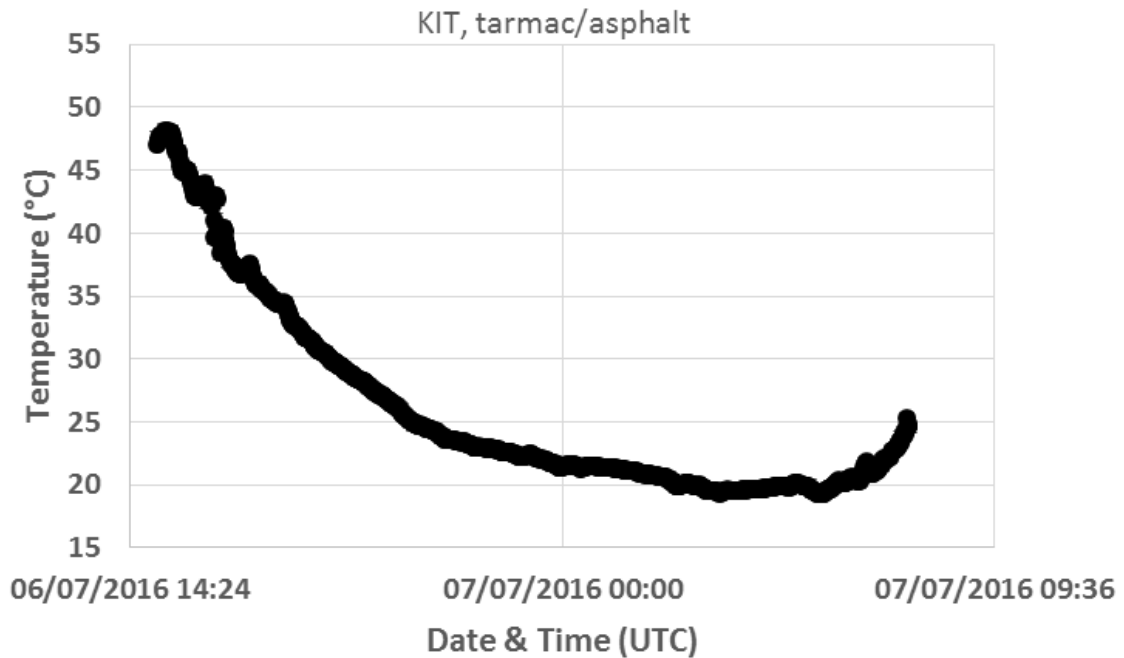

Figure 16: Surface temperature of tarmac measured by KIT on the 7th July

3.4 LST MEASUREMENTS PROVIDED BY ONERA

Institute/organisation: ONERA
2, avenue Edouard Belin – 31055 Toulouse Cedex4 - France.
Contact Name: Laurent Poutier
Email: laurent.poutier@onera.fr

ONERA provided three radiometers for the LST comparison at NPL. The ONERA-A and ONERA-B radiometers were identical (Heitronics KT19.85 II), but were used at different distances (heights) from the surface of the samples they measured. ONERA-A as located at 4 m from the ground while ONERA-B was positioned at 2.3 m above the ground. The third spectroradiometer (ONERA-C) was used to measure the emissivity of the samples.

3.4.1   Radiometers ONERA-A and ONERA-B:

Type: Heitronics KT19.85 II
Field of View: 95 mm target diameter at a 2 m range.
Spectral band: 9.6 μm to 11.5 μm
Temperature resolution: ±0.06 °C
2-sigma uncertainty: ±0.5 °C+0.7 % of the difference between target and housing
                                   temperature

The calibration of these radiometers was checked using the Mikron M345 blackbody, at two specific set temperatures.

The primary calibration error of measurements made by these radiometers is the one given by the manufacturer (±0.5 °C + 0.7 % of the difference between target and housing temperature). The RMS difference between the Mikron set temperature and the radiometer output calculated over the 14 datasets acquired in the temperature range of 12 °C to 55 °C lead to a typical difference below 0.1 K for these radiometers. Therefore, if we consider that this setup can be modelled as a blackbody surrounded by reflective coatings, so that the error in the Mikron source is limited to its temperature accuracy (equal to 0.1 K), then the primary calibration error could be decreased down to $\sqrt{2}\times0.1$ or approximately 0.15 K. This ideal modelling is probably optimistic and the final primary calibration error is consequently higher, but it could be less than the manufacturer's estimation.

Finally, the combined uncertainty of the measurements made by the ONERA-A and ONERA-B radiometers during the 2016 LST measurement comparison at the NPL is given in Table 3.4.1.

Table 3.4.1: Uncertainty contribution for the Heitronics KT19 radiometers.

Uncertainty Contribution	Type A Uncertainty in Value / %	Type B Uncertainty in Value / (appropriate units)	Uncertainty in Brightness temperature K
Repeatability of measurement	±0.05K		±0.05K
Reproducibility of measurement			<0.05K
Primary calibration		±0.5°C+0.7% ×$\Delta T_{target\text{-}inst}$	±0.5°C+0.7% ×$\Delta T_{target\text{-}inst}$
Linearity		0.02K	
RMS total			

3.4.2 The ONERA-C spectroradiometer

Type:	Spectroradiometer BOMEM MR354SC
Detector Type:	MCT Photoconductive
Spectral response:	3 to13μm @ 4 cm^{-1}
FOV:	20° full angle
Scan rate:	34 scan/s
Objective:	None

Outline technical description of the instrument: The spectroradiometer is a Michelson FTIR instrument with two Stirling-cooled detectors which allows it to cover the 3 μm to 13 μm spectral range.

The instrument output is a raw interferogram expressed in Volts as a function of the optical path difference. The spectroradiometer is very sensitive to its internal temperature, especially the beamsplitter temperature, which is maintained around 20 °C above ambient temperature. The calibration is done with the ONERA Mikron M345 4-inch by 4-inch aperture blackbody. The radiance spectrum is processed using the two reference acquisitions corresponding to the two Mikron set temperatures and the interferogram of the test source. The uncertainty is estimated by summing up the following uncertainty sources.

Sources of uncertainty considered for the error budget.

Blackbody temperature short term stability	±0.04 K (dependent on the reference measurement)
Blackbody temperature accuracy	±0.1 K (bias common to the 2 reference measurements)
Blackbody emissivity accuracy	±0.01
Skin Bomem temperature uncertainty	±4 K

The overall uncertainty is shown in Table 3.4.2, for the different experiment temperatures. Logically, when extrapolating regarding the calibration values, the uncertainty grows. The

retrieved brightness temperature tends to exhibit a noticeable spectral signature when the measured temperature is outside the calibration interval. This extrapolation behaviour is probably due to the non-linearity of the detector and/or issues with the calibration source model.

Table 3.4.2: Calibration temperatures and estimated uncertainty for the brightness temperatures derived from the Bomem spectroradiometer.

Set temperature of the experiment	Calibration first temperature (°C)	Calibration second temperature (°C)	RMS uncertainty for the brightness temperature (K)
-15	12	45	0.4
0	15	40	0.3
10	15	40	0.24
20	15	40	0.2
30	20	40	0.19
45	30	55	0.2

3.4.3 LST measurement at NPL

3.4.3.1 Spectral emissivity measurement set-up

The spectral emissivity was derived from 2 radiance spectra measured sequentially: one looking down at the sample, the other one looking at a diffuse reflector, in order to estimate the downwelling irradiance. The spectra were acquired by the ONERA-C, BOMEM MR304SC FTIR spectroradiometer equipped with a 75 mrad FoV telescope and a 45° flat mirror. With this setup, the ground target surface was viewed at nadir and the diameter of the analysed area was approximately 15 cm. The reflector was a Labsphere Infragold 10"x10" standard.

The two acquisitions are done sequentially within typically 30 s. The temporal variations of the atmospheric conditions were assumed negligible in this time interval, even for the broken clouds sky conditions that were encountered most of the time. The radiometric calibration used 2 acquisitions of the same MIKRON M345 4"x4" blackbody set at two different temperatures, done before and after the measurements. For these measurements, the flat mirror was tilted and the blackbody active surface was vertical. The blackbody emissivity was assumed to be spectrally constant. Its nominal value was set to 0.98. The reflective contribution was supposed to come from an environment at a brightness temperature equal to the ambient temperature, given by a RTD sensor.

The method was applied to the six different samples of the study. An error budget was evaluated by considering the error sources shown Table below:

Blackbody temperature short term stability: ±0.04 K
Blackbody temperature accuracy: ±0.1 K
Blackbody emissivity accuracy: ±0.01
Ambient temperature uncertainty   ±3 K
Reflector reflectance uncertainty   ±0.02
Reflector surface temperature uncertainty   ±2 K

3.4.4. LST Measurements completed by the ONERA-A radiometer

Figures 17, 18, 19, 20, 21 and 22 show the measurements completed by ONERA-A radiometer on clover, short grass, gravel, sand, soil and tarmac/asphalt, respectively. The uncertainty bars in the figures represent the uncertainty values provided by ONERA which correspond to the measurements shown in the Figures.
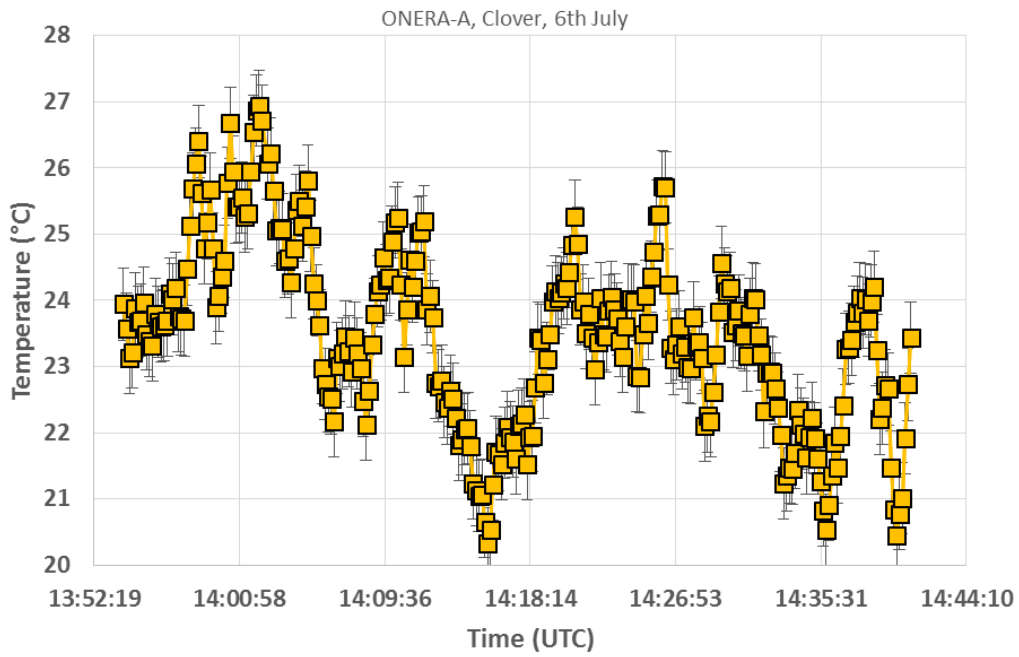

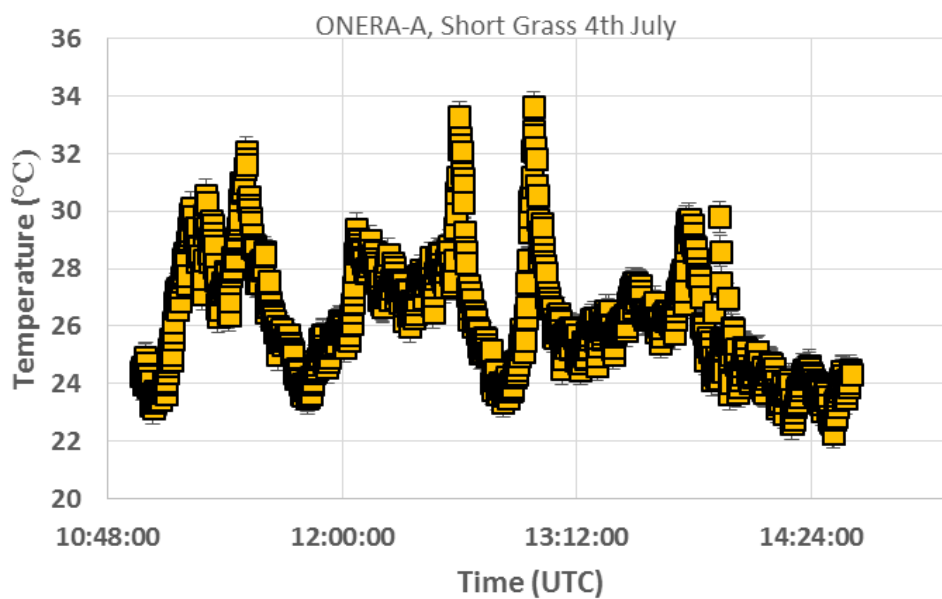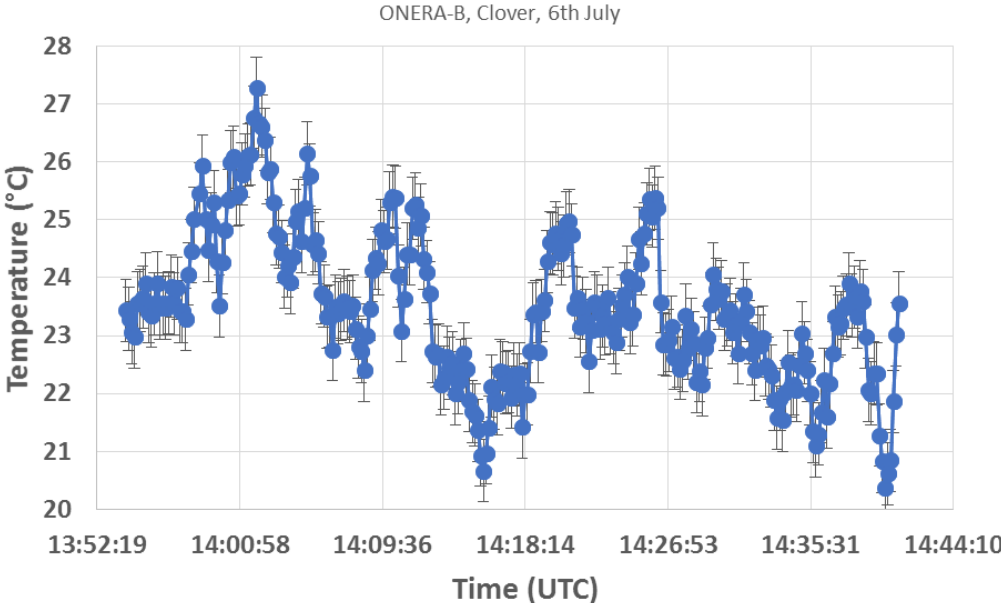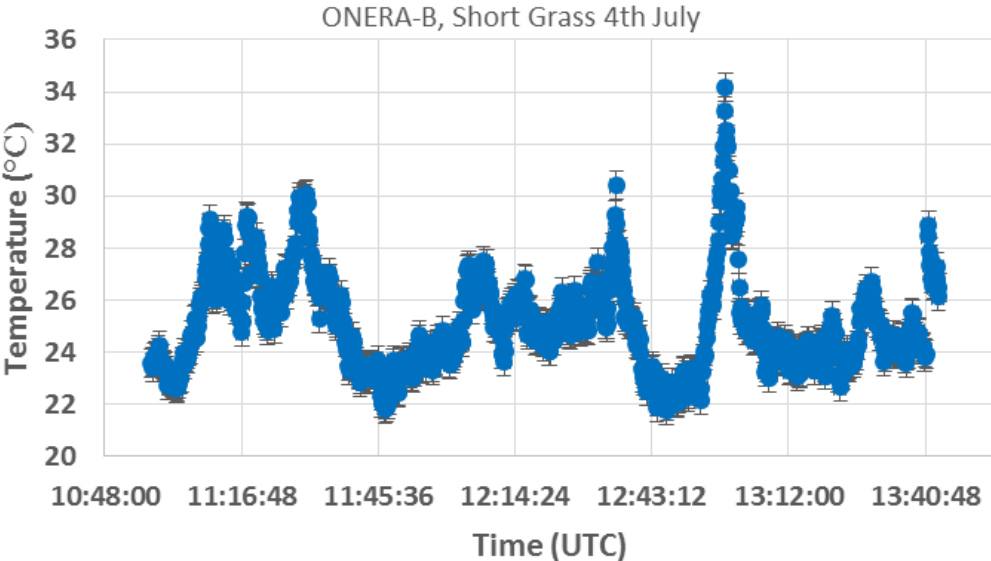Figure 17: Surface temperature of clover measured by the ONERA-A radiometer on the 6th July 2016

Figure 18: Surface temperature of short grass measured by the ONERA-A radiometer on the 4th July 2016
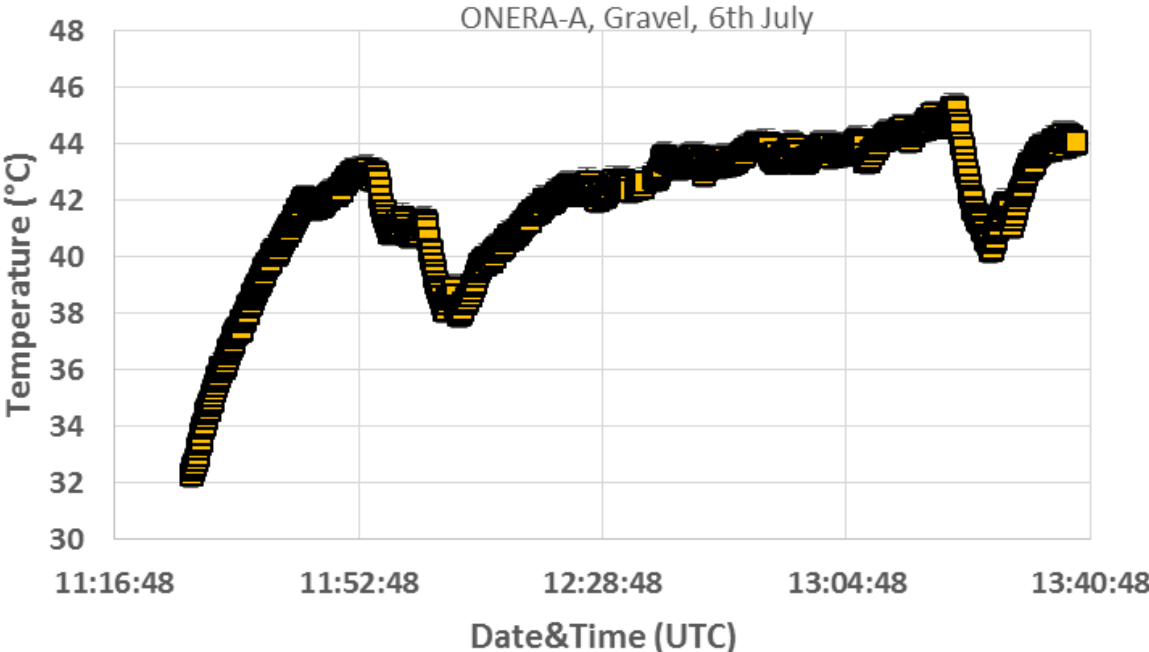
Figure 19: Surface temperature of gravel measured by the ONERA-A radiometer
on the 6th July 2016
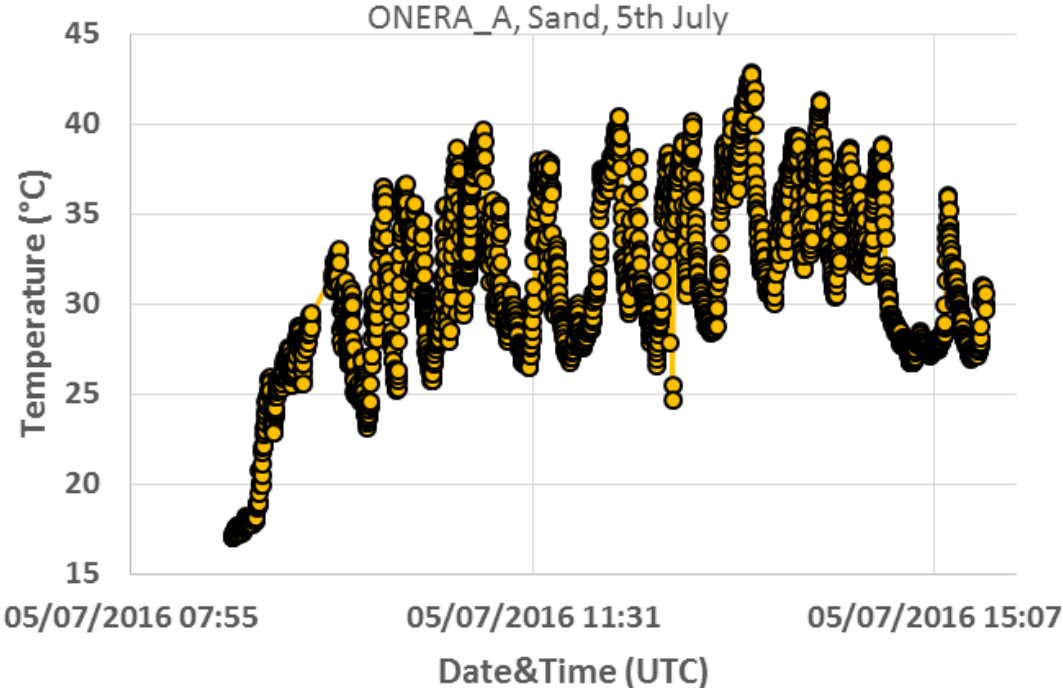
Figure 20: Surface temperature of sand measured by the ONERA-A radiometer on the 5th July
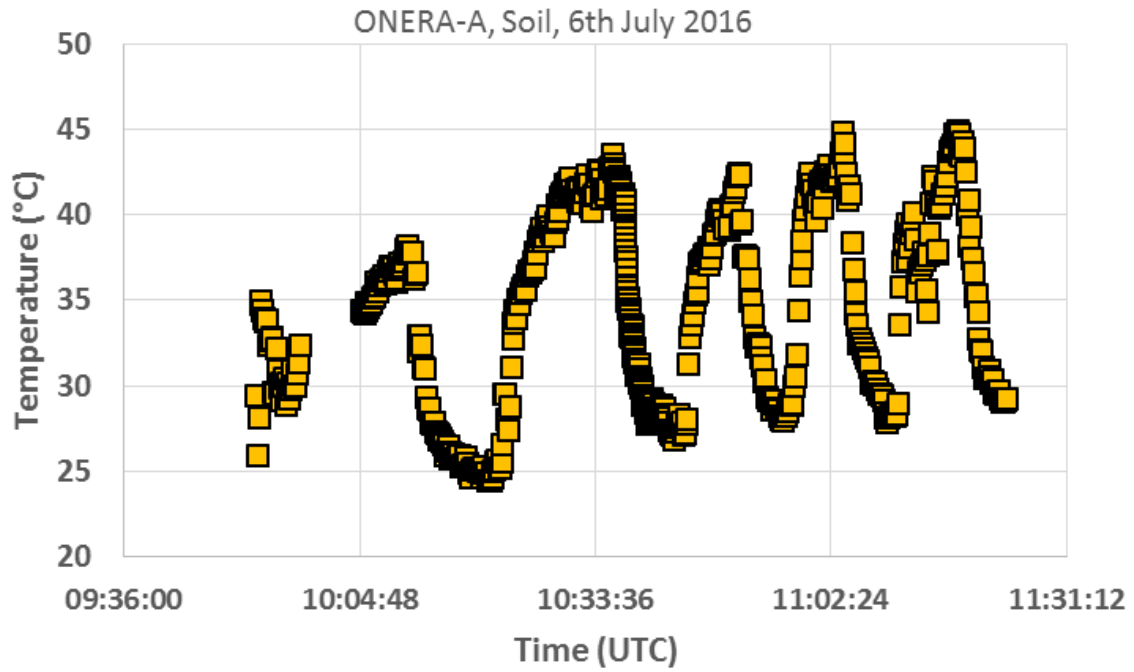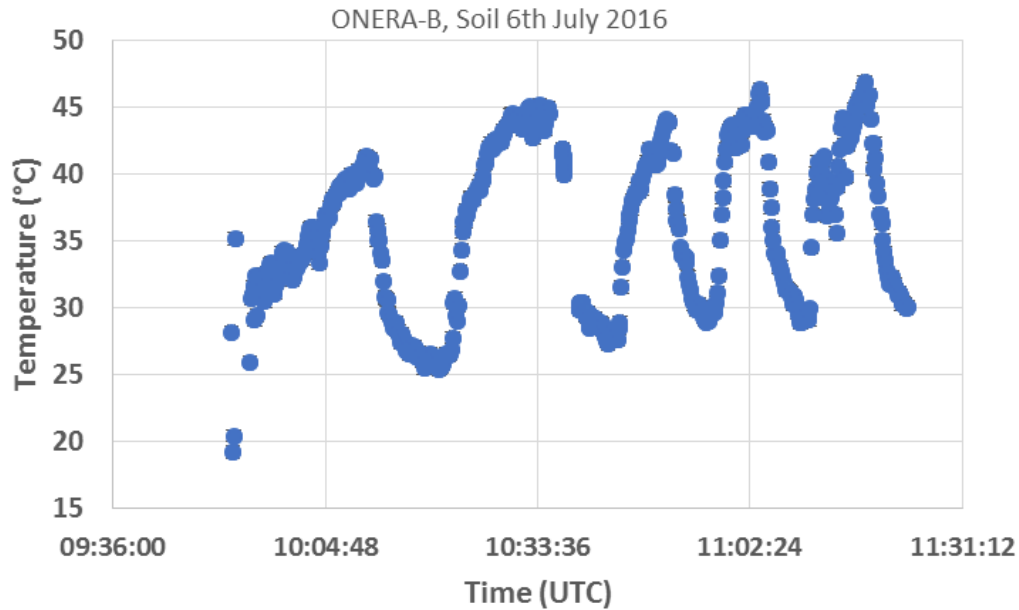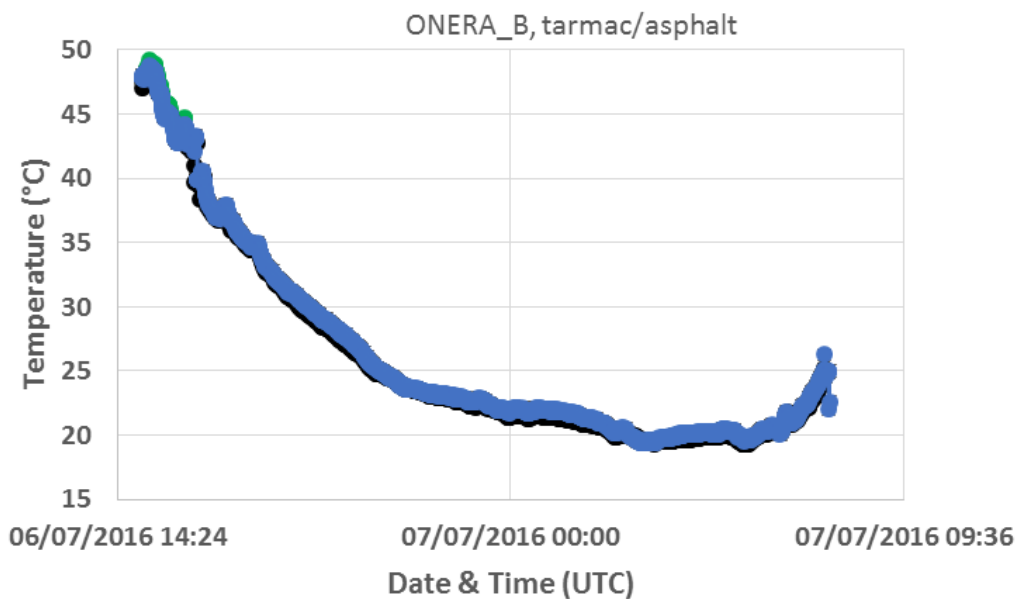
Figure 21: Surface temperature of soil measured by the ONERA-A radiometer on the 6th July
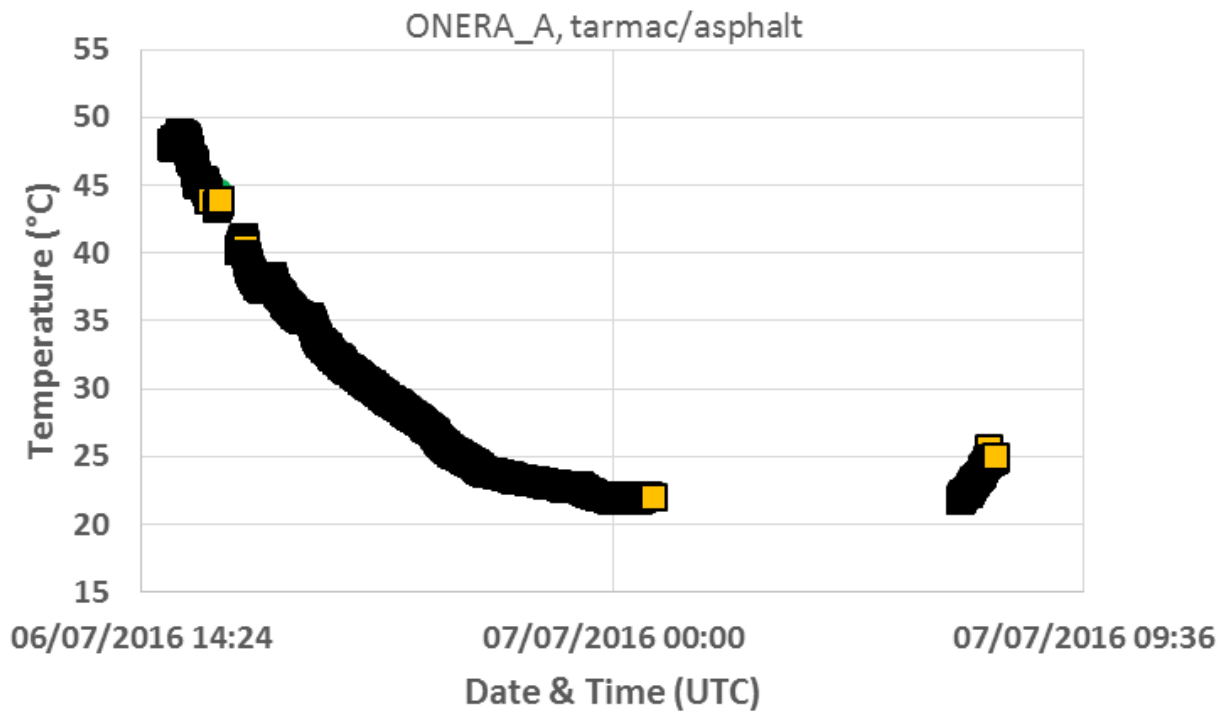
Figure 22: Surface temperature of tarmac measured by ONERA-A radiometer
on the 6th and 7th July 2016.

3.4.5 LST Measurements completed by the ONERA-B radiometer

Figures 23, 24, 25, 26 27 and 28 show the measurements completed by the ONERA-B radiometer on clover, short grass, gravel, sand, soil and tarmac/asphalt, respectively. The uncertainty bars in the figures represent the uncertainty values provided by ONERA which correspond to the measurements shown in the Figures.

Figure 23: Surface temperature of clover measured by ONERA-B on the 6th July

Figure 24: Surface temperature of short grass measured by ONERA-B on the 4th July
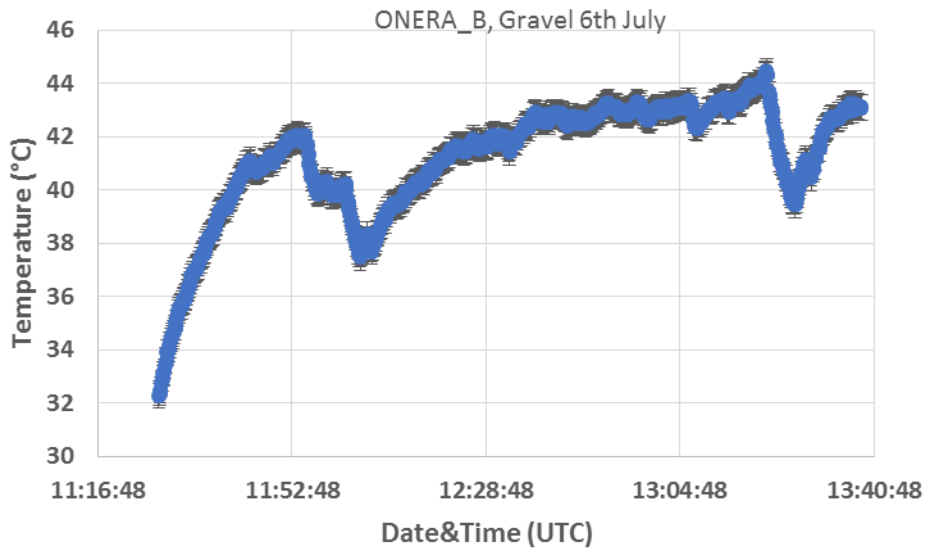
Figure 25: Surface temperature of gravel measured by ONERA-B on the 6th July
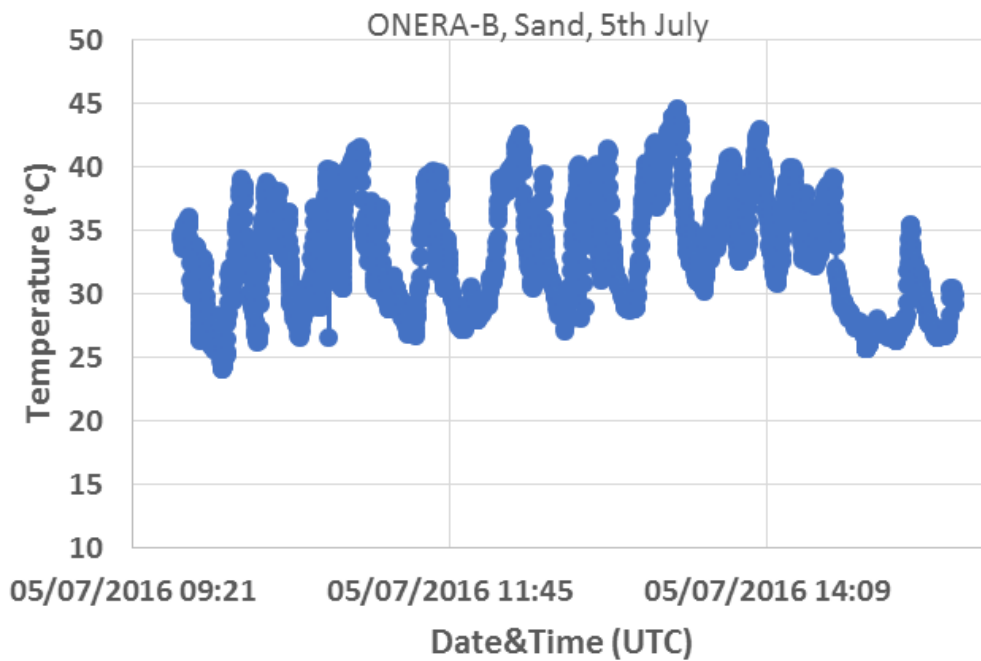
Figure 26: Surface temperature of sand measured by ONERA-B on the 5th July

Figure 27: Surface temperature of soil measured by ONERA-B on the 6th July

Figure 28: Surface temperature of tarmac measured by ONERA-B on the 6th and 7th July

4.   COMPARISON OF LAND SURFACE TEMPERATURE (LST) MEASUREMENTS

Section 4 provides a comparison of the measurements completed by the radiometers participating in the 2016 FRM4STS LST comparison at NPL. A total of five radiometers participated in the LST comparison which took place at NPL from 4th July to 8th July 2016.

Participants provided their measurements at different times. In order to be able to compare their measurements, a standard interpolation method was used to estimate the measurements of the different participants at 10 second time intervals.

Land surface temperature measurements should ideally be compared to a mean, determined from the measurements of the radiometers, weighted by their uncertainties. However, to do this requires a full breakdown of uncertainties so that the weights can be fully evaluated and agreed upon by participants in advance. This was not possible from the data provided by some participants. An alternative approach was adopted which uses the simple mean of the radiometer measurements.

In reviewing the data, no consideration was also made as to potential differences between night and day.

4.1 MEASUREMENTS ON THE SHORT GRASS SAMPLE

The surface temperature of the short grass was measured on the 4th July. Figures 29 and 30 show combinations of thermal images of the sample with black and white, visible images of the target. The Figures show that the apparent surface temperature of the sample was varying by about 5 ºC over the measured area. The variation in temperature is due to a combination of true temperature changes due to the difference of the temperature of the sample and the air temperature as well as due to spatial emissivity variations on the surface of the sample.
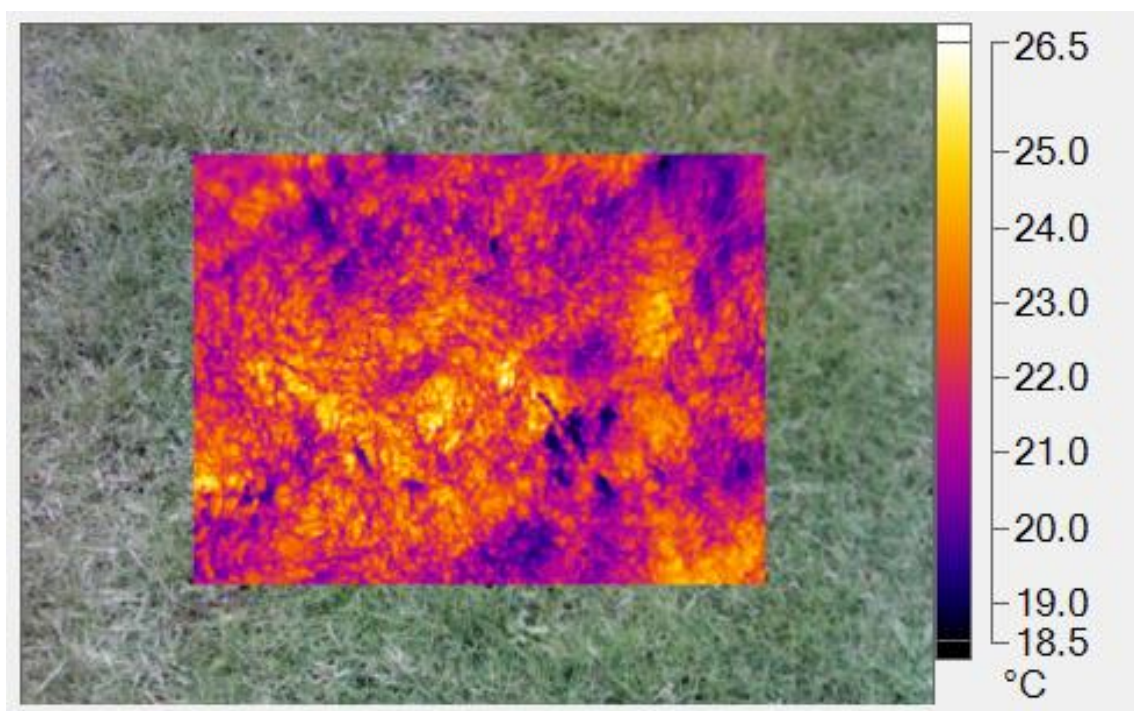
Figure 29: Combination of a thermal image of the short grass sample with a black and white, visible image of the same target. The Figure shows that the apparent surface temperature of the sample was varying by about 5 ºC over the measured area.
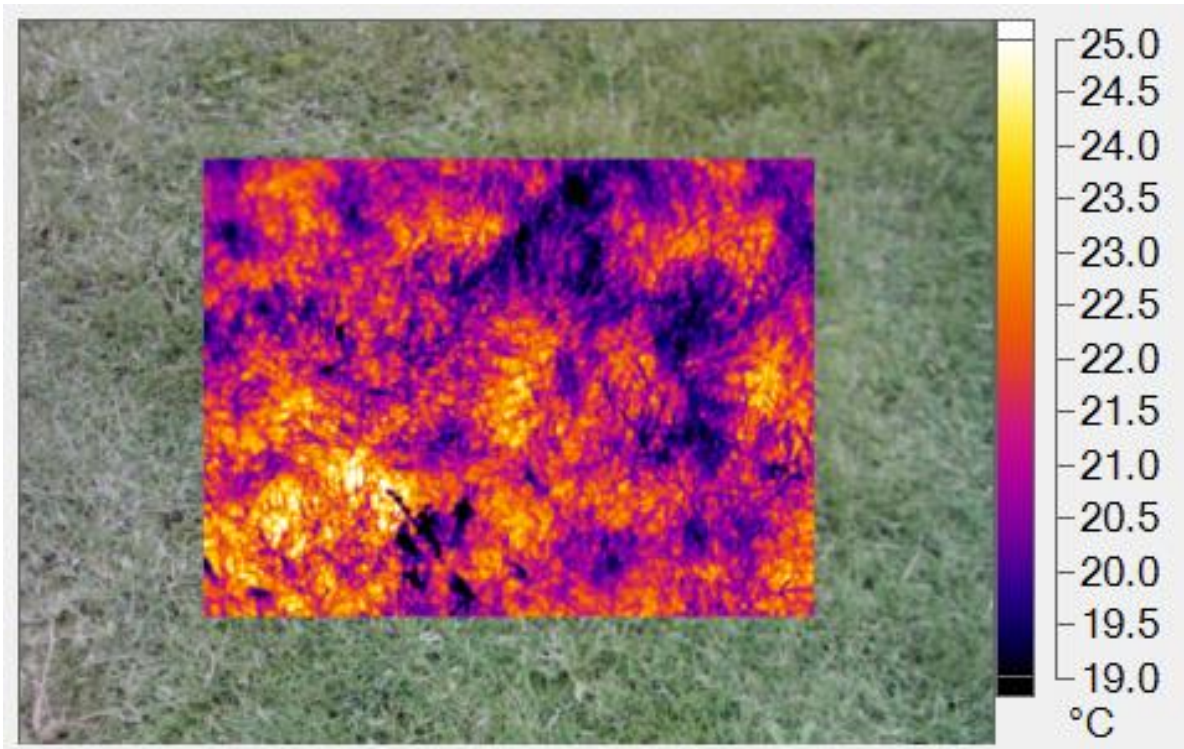
Figure 30: Another image of the combination of a thermal image of the short grass sample with a black and white, visible image of the same target. The Figure shows that the apparent surface temperature of the sample was varying by about 5 $^{\circ}$C over the measured area.

Figure 31 shows the measurements reported by the different participants over the five hour monitoring period. Figure 32 shows the difference of the measuring radiometers from their mean. Because participants provided their measurement at different times, a standard interpolation method was used to estimate the measurements of the different participants at 10 second intervals. Figure 32 shows that the bulk of the measurements exhibit a difference of all four radiometers from their mean of within ±3 $^{\circ}$C. Finally, Figure 33 shows the difference between the surface temperature of the short grass sample measured by participants and the mean of the measurements of all participants.
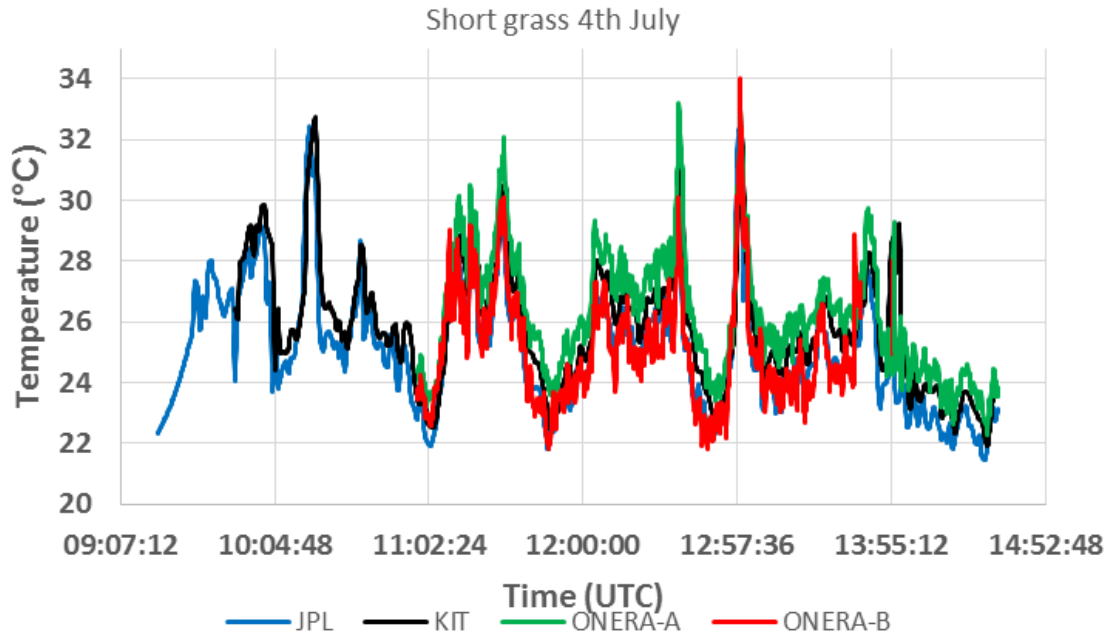
Figure 31: Surface temperature of short grass sample measured using the participating radiometers on the 4th July 2016.
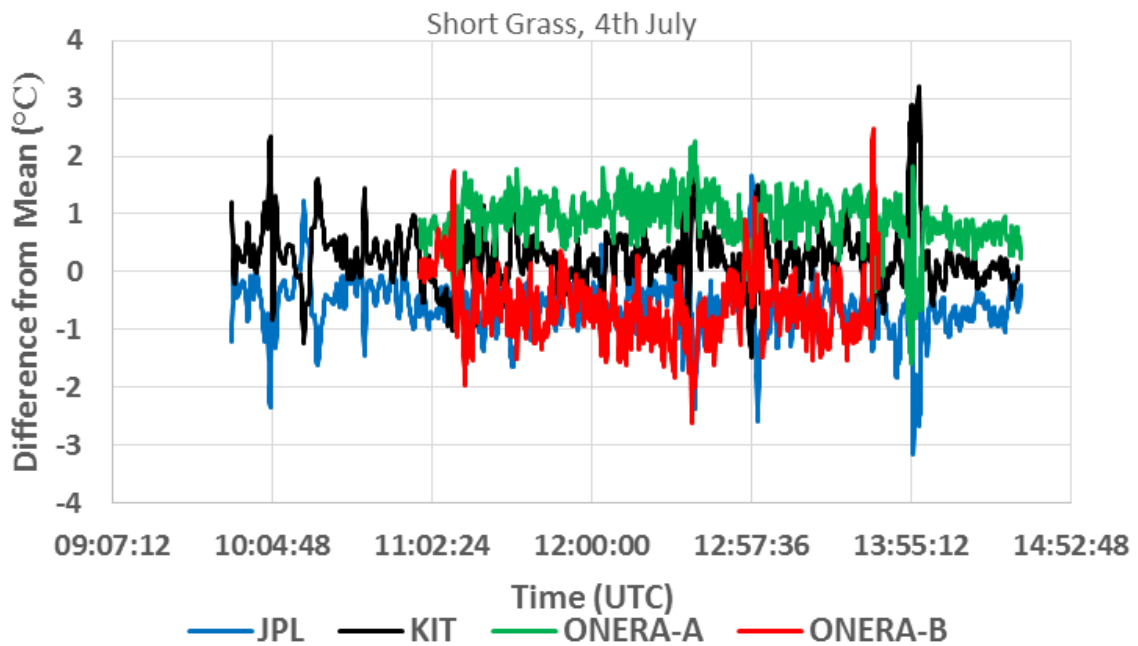
Figure 32: Difference between the measurements using each of the four measuring radiometers for the short grass sample and their mean. This Figure shows that the difference of all four radiometers from their mean is within ±3 ^{o}C throughout the monitoring period.
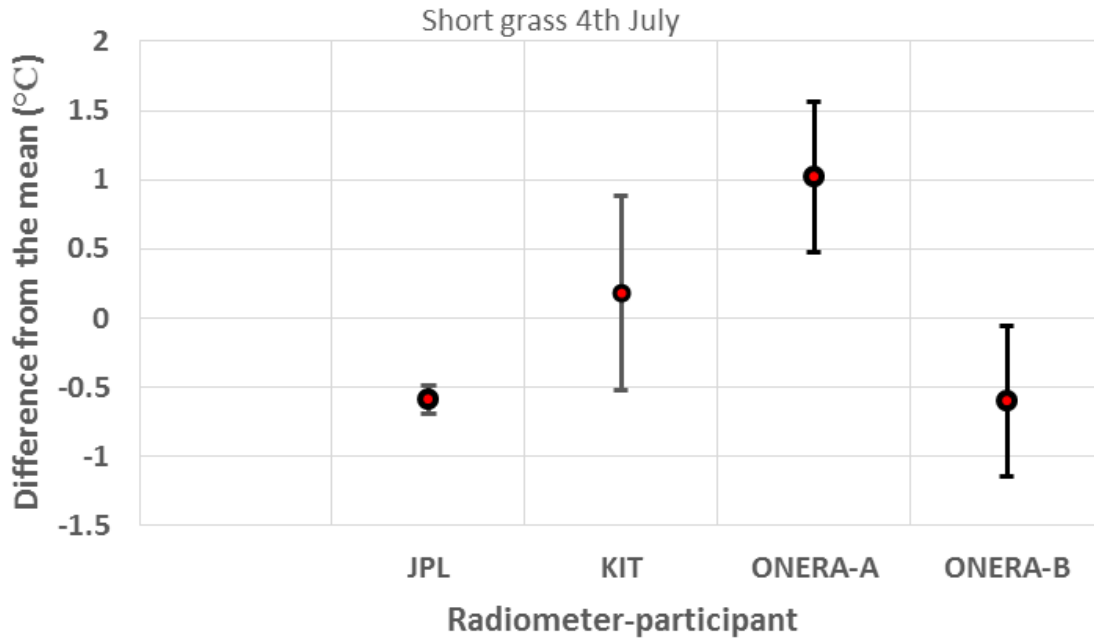
Figure 33: Difference between the mean surface temperature of the short grass sample measured by participants and the mean of the measurements of all the participants.

4.2 MEASUREMENTS ON THE CLOVER SAMPLE

The surface temperature of the clover sample was measured on the 6th July. Figure 34 shows a combination of a thermal image of the sample with a black and white, visible image of the target. It shows that the apparent surface temperature of the sample was varying by about 10 $^\circ$C over the measured area. The variation in temperature is due to a combination of true temperature changes due to the difference of the temperature of the sample and the air temperature as well as due to spatial emissivity variations on the surface of the sample.

Figure 35 shows the measurements reported by the different participants on the surface temperature of the clover sample. Peak-to-peak fluctuation in the surface temperature of the clover sample of about 7 $^\circ$C was observed during the measurement period. Figure 36 shows the difference between the measurements obtained using each the five measuring radiometers and their mean. Because participants provided their measurement at different times, a standard interpolation method was used to estimate the measurements of the different participant at 10 second intervals. Figure 36 shows that the difference of all five radiometers from their mean is within ± 1.5 $^\circ$C throughout the monitoring period. Finally, Figure 37 shows the difference between the surface temperature of the clover sample measured by participants and the mean of the measurements of all participants.
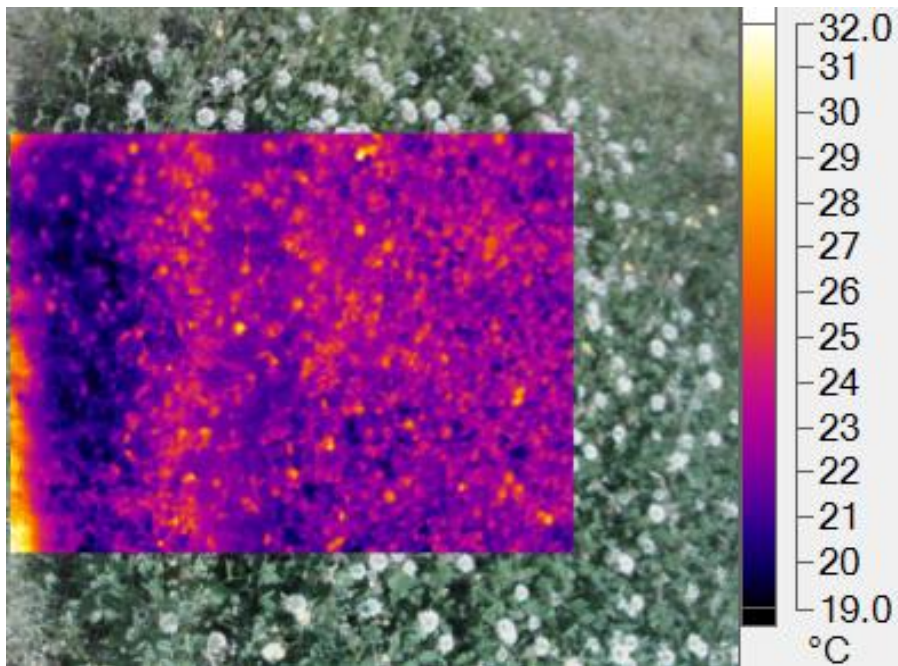
Figure 34: Combination of a thermal image of the clover sample with a black and white, visible image of the same target. The Figure shows that the apparent surface temperature of the sample was varying by about 10 °C over the measured area.
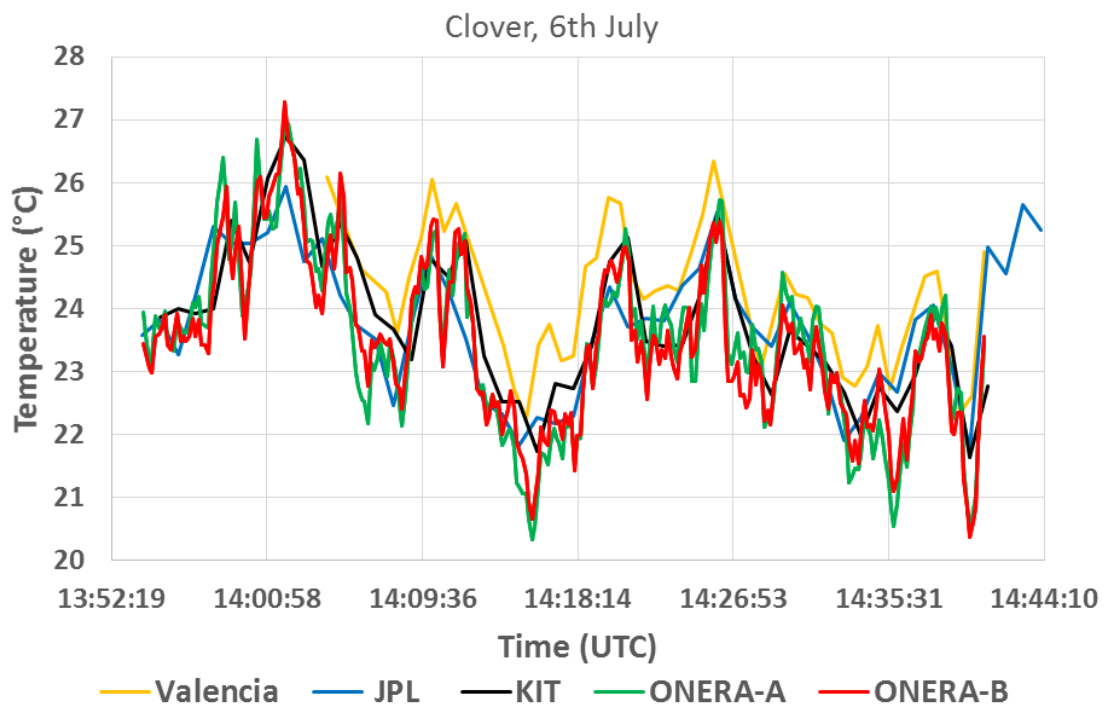

Figure 35: Surface temperature of the clover sample measured using the participating radiometers on the 6th July 2016.
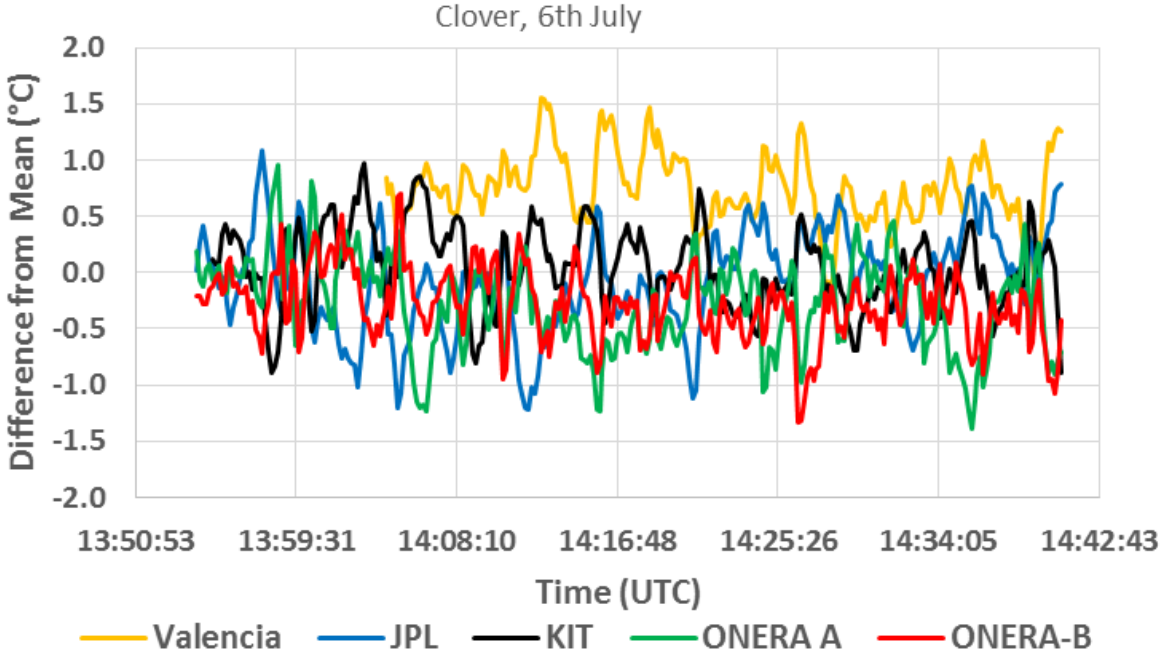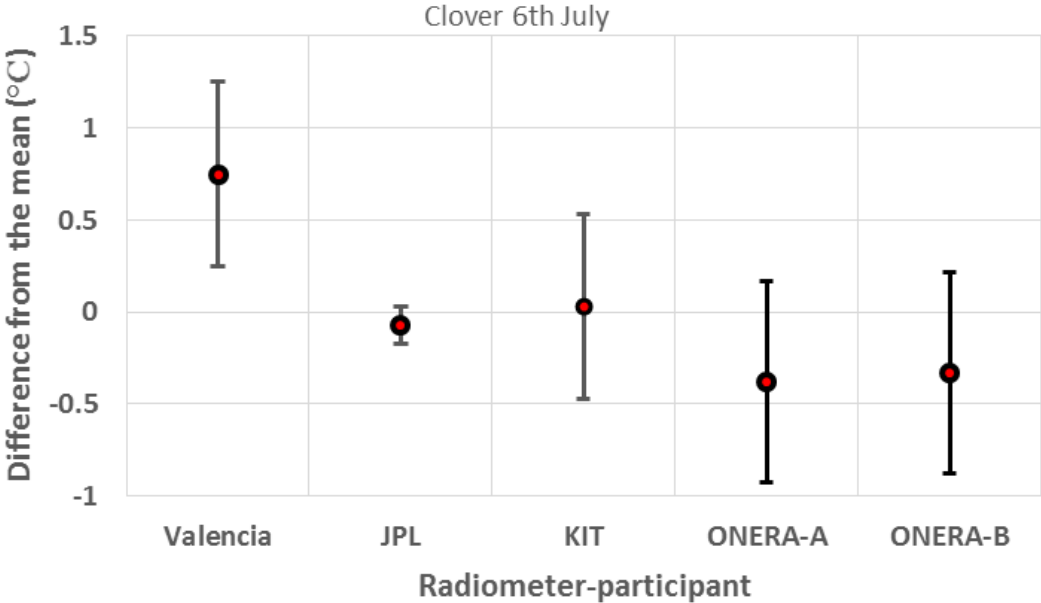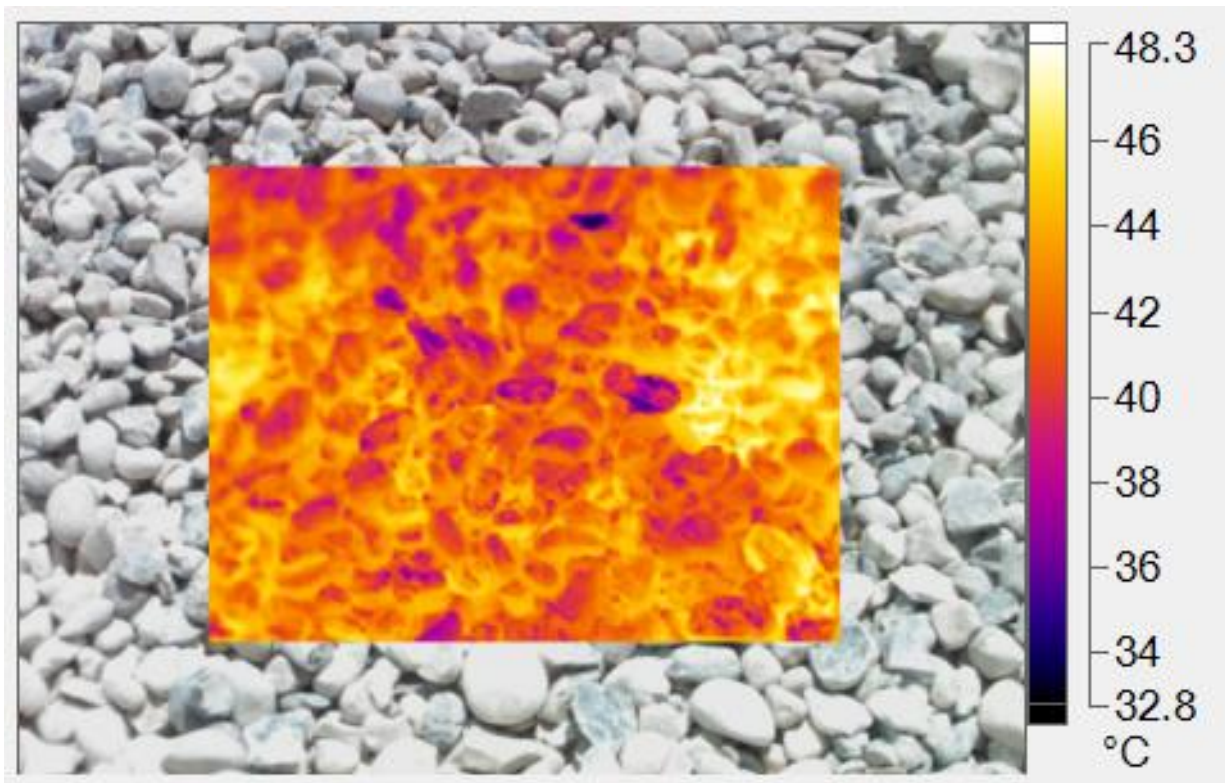
Figure 36: Difference between the measurements using each of the five measuring radiometers for the clover sample and their mean. This Figure shows that the difference between all five radiometers and their mean is within ±1.5 °C throughout the monitoring period.

Figure 37: Difference between the mean surface temperature for the clover sample measured by participants and the mean of the measurements of all the participants.

4.3 MEASUREMENTS ON THE GRAVEL SAMPLE

The surface temperature of gravel was measured on the 6th July. Figure 38 shows a combination of a thermal image of the sample with a black and white, visible image of the target. It shows that the apparent surface temperature of the sample was varying by about 10 ^{o}C over the measured area. The variation in temperature is due to a combination of true temperature changes due to the difference of the temperature of the sample and the air temperature as well as due to spatial emissivity variations on the surface of the sample.

Figure 38: Combination of a thermal image of the gravel/pebble sample with a black and white, visible image of the same target. The Figure shows that the apparent surface temperature of the sample was varying by about 10 ^{o}C over the area of the measured sample.

Figure 39 shows the measurements reported by the five participants. Figure 40 shows the difference between the five measuring radiometers and their mean. Because participants provided their measurement at different times, a standard interpolation method was used to estimate the measurements of the different participants at 10 second intervals.The Figure shows that the difference between the measurements of all five radiometers and their mean is within ±2 ^{o}C. Finally, Figure 41 shows the difference between the mean surface temperature of the gravel sample measured by participants and the mean of the measurements of all the participants.
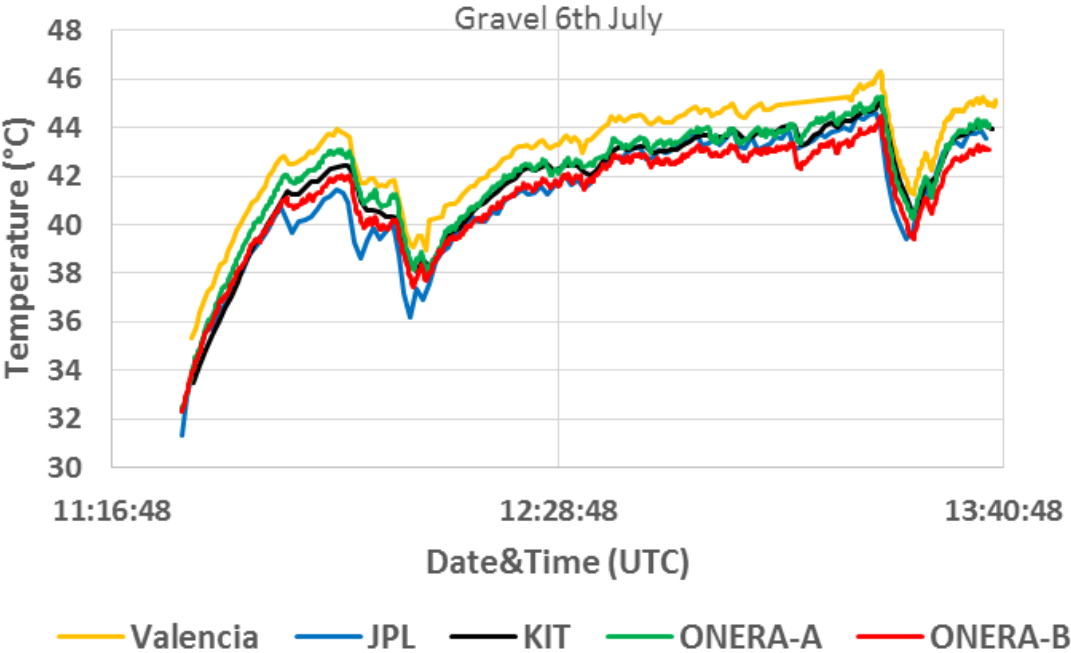
Figure 39: Surface temperature of gravel measured using the participating radiometers on the 6th July 2016.
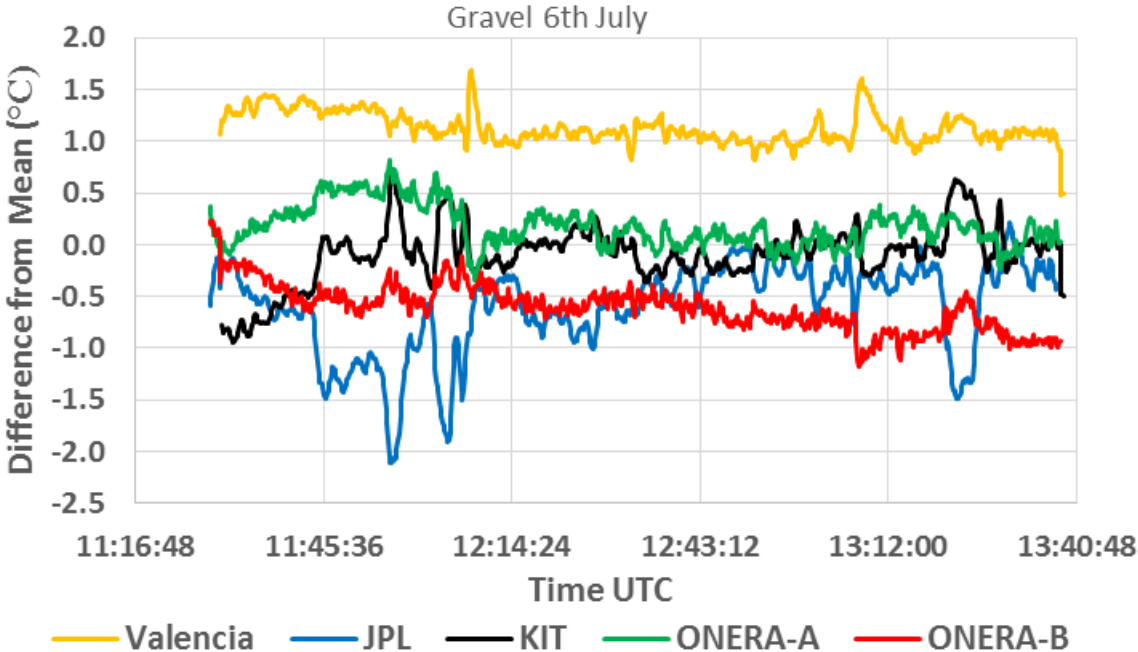

Figure 40: Difference between the measurements using each the five measuring radiometers for the gravel sample and their mean. This Figure shows that the difference between all five radiometers and their mean is within ±2 °C throughout the monitoring period.
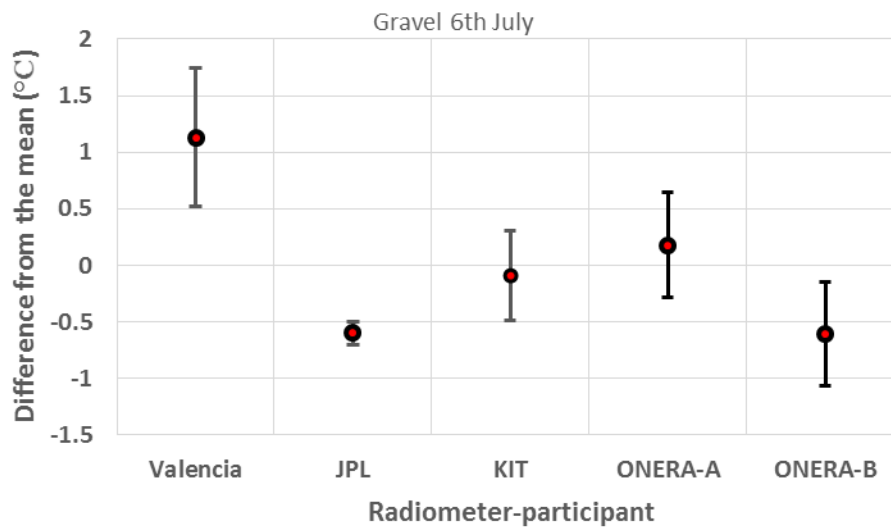
Figure 41: Difference between the surface temperature of the gravel sample measured by participants and the mean of the measurements of all participants.

4.4 MEASUREMENTS ON THE DARK SOIL SAMPLE

The surface temperature of the dark soil was measured on the 6th July. Figure 42 shows a combination of a thermal image of the sample with a black and white, visible image of the target. It shows that the apparent surface temperature of the sample was varying by about 10 ºC over the measured area. The variation in temperature is due to a combination of true temperature changes due to the difference of the temperature of the sample and the air temperature as well as due to spatial emissivity variations on the surface of the sample.
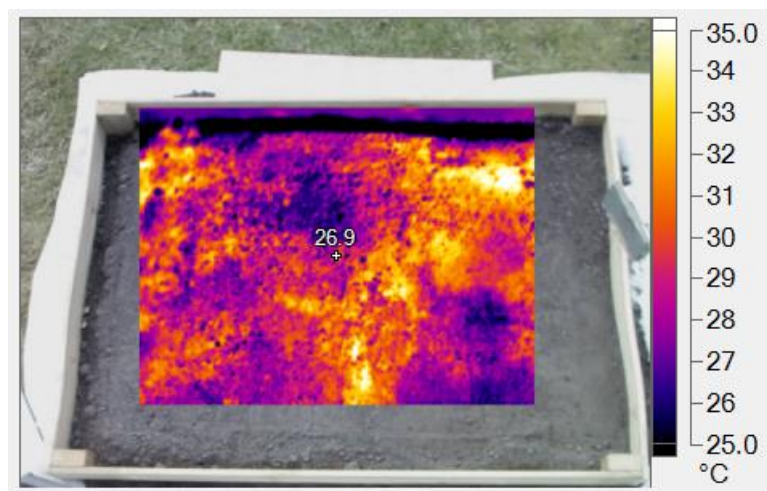

Figure 42: Combination of a thermal image of the dark soil sample with a black and white, visible image of the same target. The Figure shows that the apparent surface temperature of the sample was varying by about 10 ºC over the measured area.

Figure 43 shows the measurements reported by the different participants over the monitoring period. Figure 44 shows the difference between the five measuring radiometers and their mean. Because participants provided their measurement at different times, a standard interpolation method was used to estimate the measurements of the different participants at 10 second intervals. The Figure shows that for the bulk of the measurements the difference between all five radiometers and their mean is within ±6 °C. Finally, Figure 45 shows the difference between the surface temperature of the dark soil sample measured by participants and the mean of the measurements of all participants.
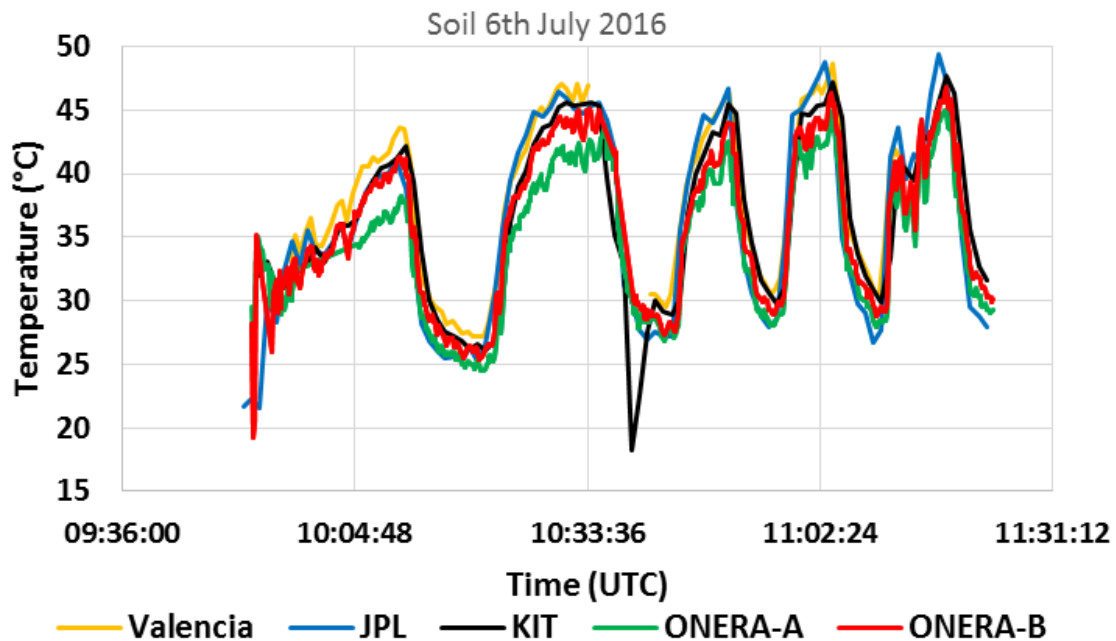

Figure 43: Surface temperature of dark soil measured using the participating radiometers on the 6th July 2016. The spike which appears at 10:39 AM on the measurements by KIT arose due to the partial obscuration of the radiometer FoV by a participant.
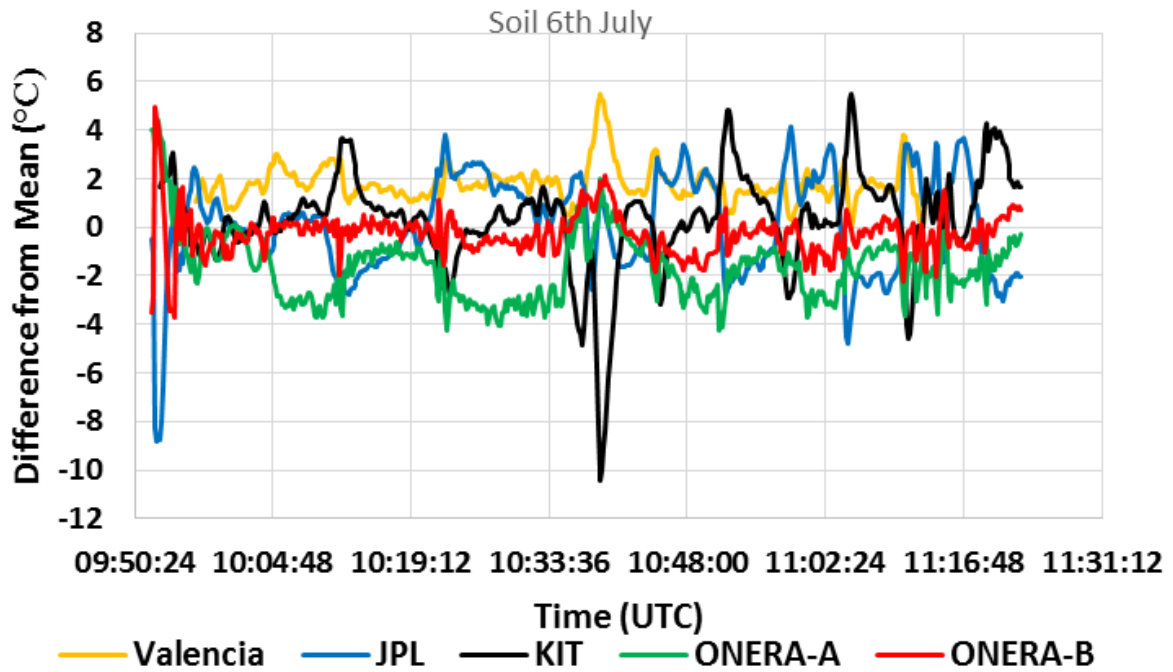
Figure 44: Difference between the measurements using each of the five measuring radiometers made on the 6th July for the dark soil sample and their mean. The spike which appears at 10:39 AM on the measurements by KIT arose due to the partial obscuration of the radiometer FoV.
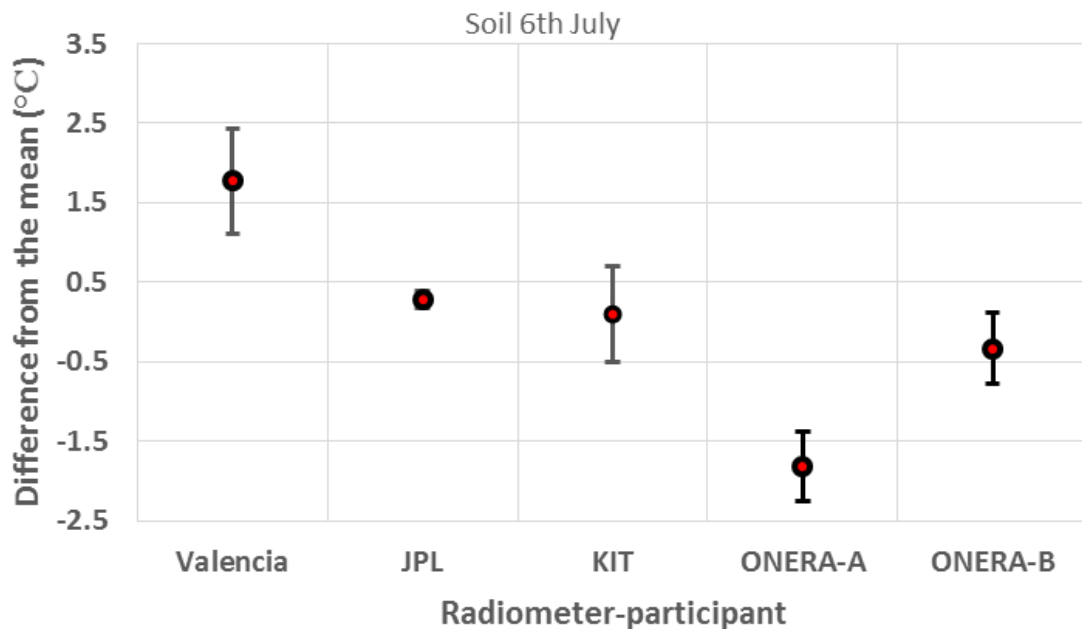

Figure 45: Difference between the surface temperature of the dark soil sample measured by participants and the mean of the measurements of all participants.

4.5   MEASUREMENTS ON THE SAND SAMPLE

The surface temperature of the sand sample was measured on the 5th and 6th July. Figure 46 shows a combination of a thermal image of the sample with a black and white, visible image of the target. It shows that the apparent surface temperature of the sample was varying by about 5 °C over the measured area. The variation in temperature is due to a combination of true temperature changes due to the difference of the temperature of the sample and the air temperature as well as due to spatial emissivity variations on the surface of the sample.
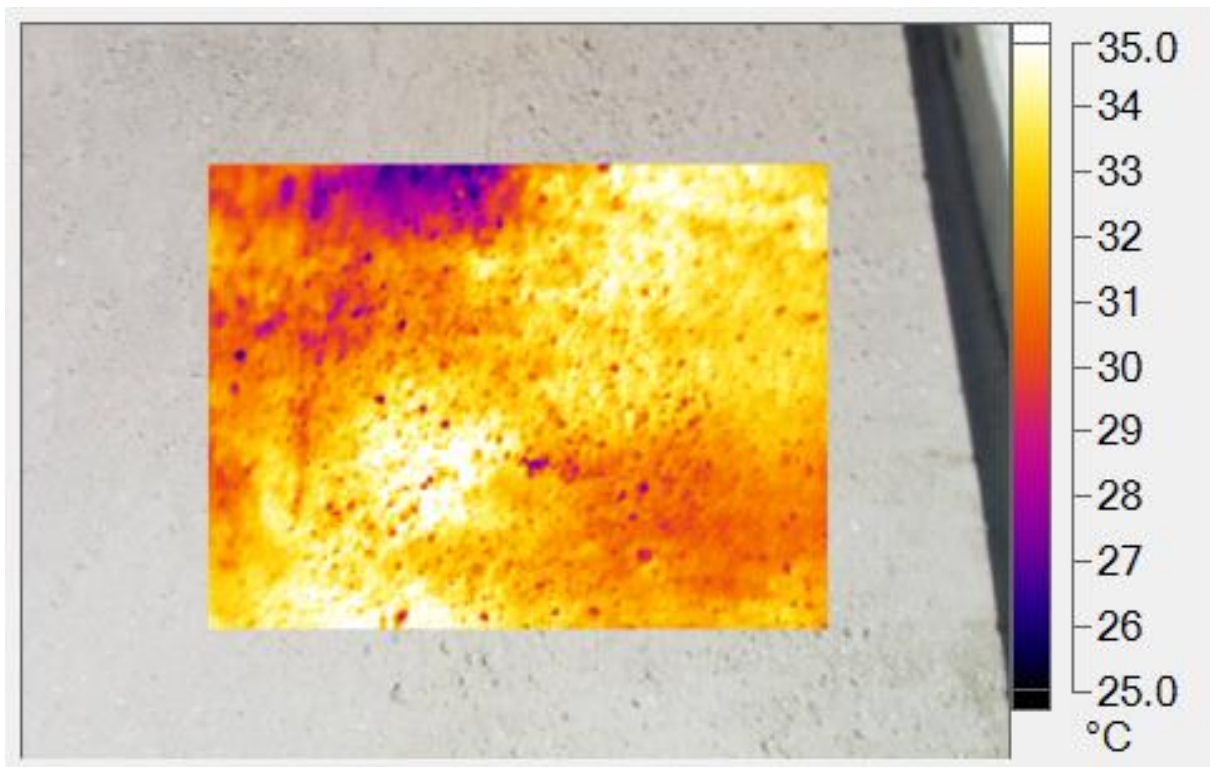

Figure 46: Combination of a thermal image of the sand sample with a black and white, visible image of the same target. The Figure shows that the apparent surface temperature of the sample was varying by about 5 °C over the measured area.

Figures 47 and 48 show the measurements reported by the different participants on the 5th and 6th July, respectively. Figures 49 and 50 show the difference between the measurements made using each of the radiometers on the 5th and 6th July and their mean, respectively. Because participants provided their measurement at different times, a standard interpolation method was used to estimate the measurements of the different participants at 10 second intervals. The Figures 49 and 50 show that the difference between all radiometers and their mean is within ±6 °C for both days during which measurements were done. Finally, Figures 51 and 52 show the difference between the surface temperature of the sand sample measured by participants and the mean of the measurements of all participants.

Figures 49 and 50 show that the measurements made with the JPL radiometer were typically 3 °C lower than corresponding measurements of other participants for both days of measurements. JPL reported that their temperature values were the raw land surface temperatures of the sand and were not adjusted for the emissivity of the sand. Furthermore, some of the sand appeared to be wet, particularly after raking the sand and based on the field-

of-view of the JPL radiometer, the moisture of the sand could have affected the temperature readings observed which might contributed to the 3 K lower temperature values.
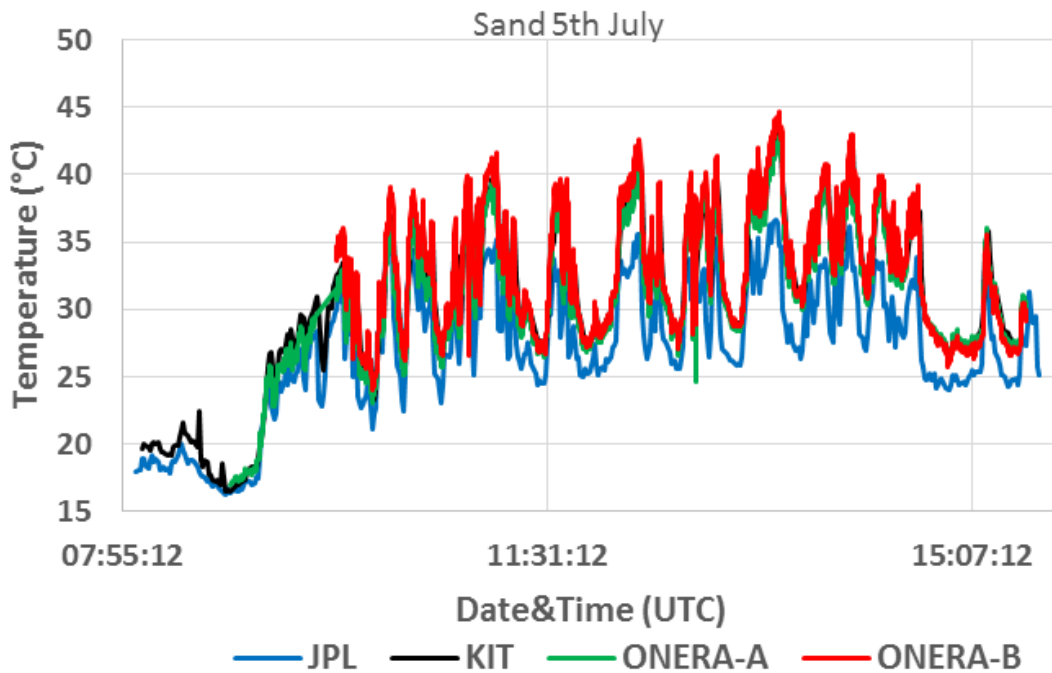

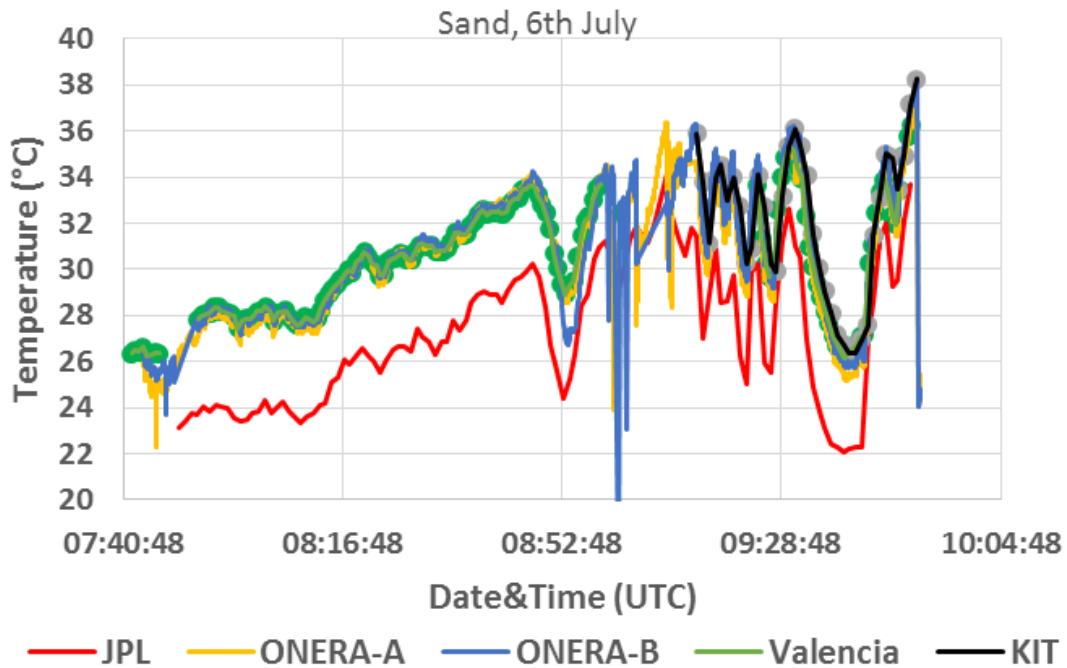Figure 47: Surface temperature of sand measured using the participating radiometers on the 5th July 2016.

Figure 48: Surface temperature of sand measured using the participating radiometers on the 6th July 2016.
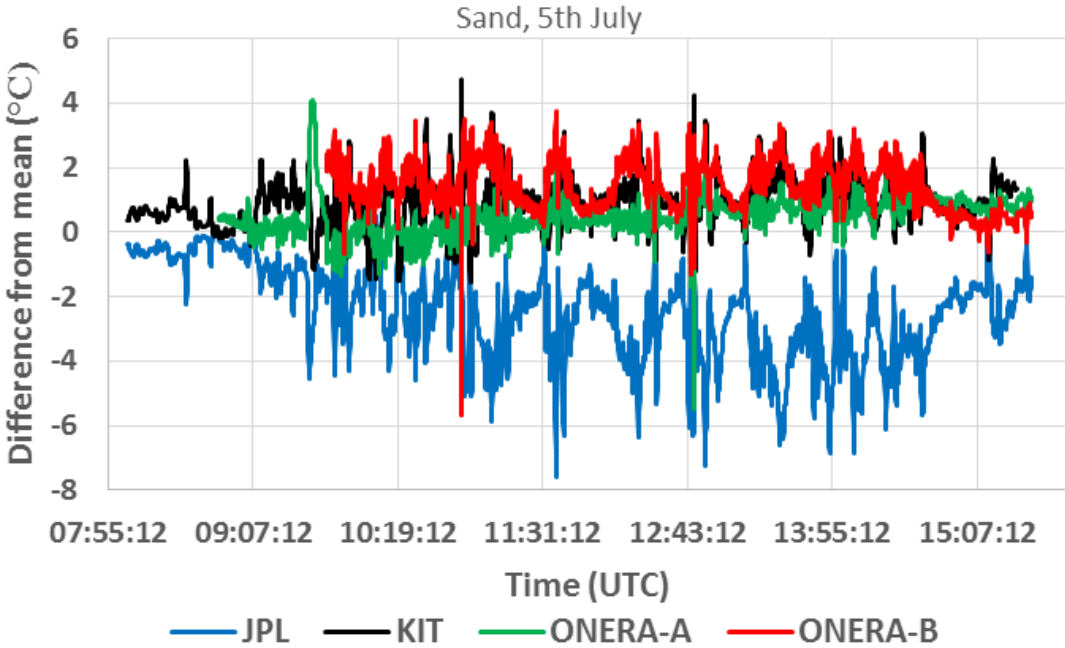
Figure 49: Difference between the measurements using each of the measuring radiometers for the sand sample and their mean recorded on 5th July.
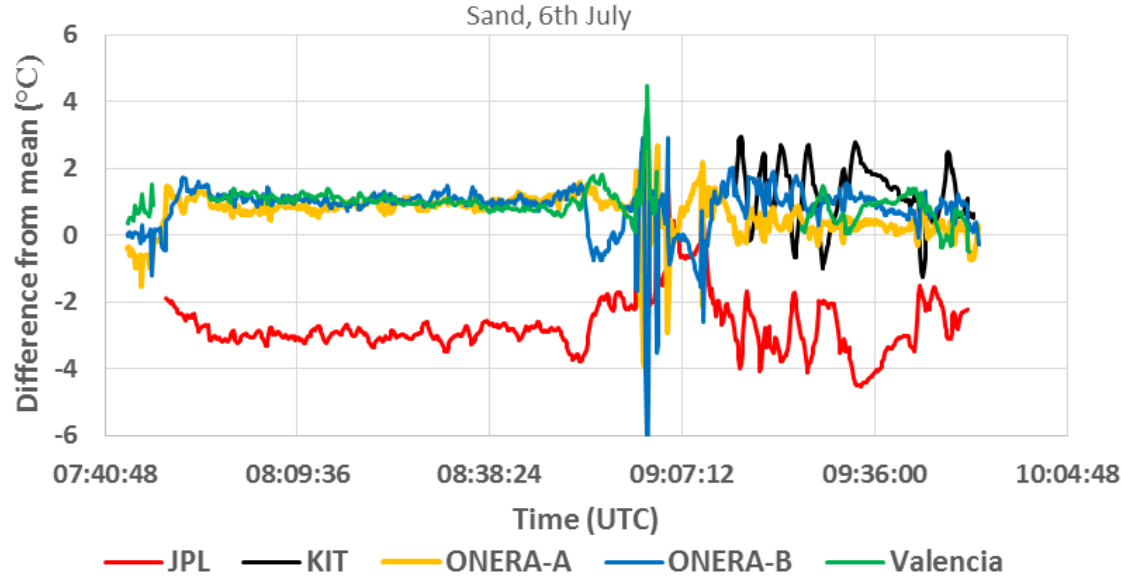

Figure 50: Difference between the measurements using each of the measuring radiometers for the sand sample and their mean, recorded on 6th July.
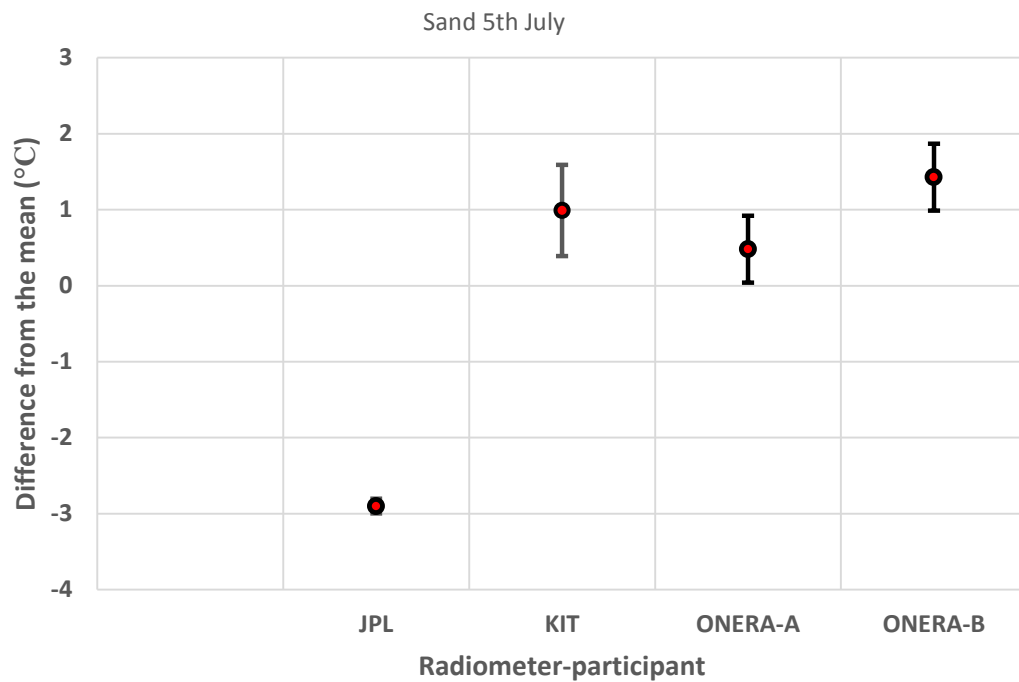
Figure 51: Difference between the surface temperature of the sand sample measured by participants on 5th July and the mean of the measurements of all participants.
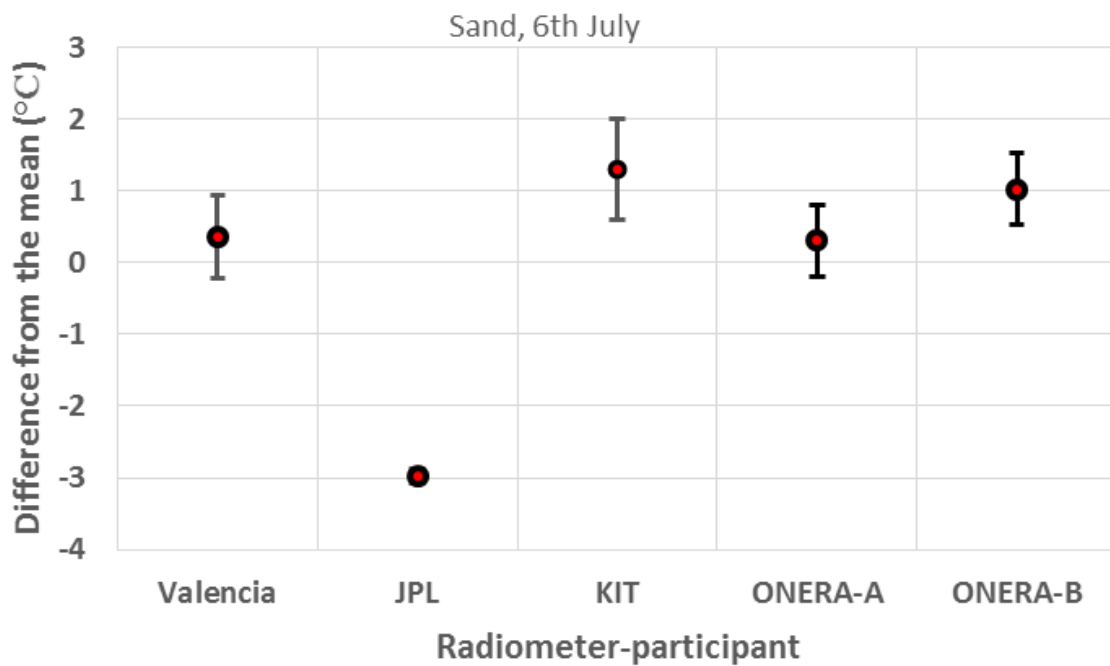

Figure 52: Difference between the surface temperature of the sand sample measured by participants on 6th July and the mean of the measurements of all participants.

4.6   MEASUREMENTS ON THE TARMAC/ASPHALT SAMPLE

The surface temperature of the tarmac/asphalt sample was measured on the 6th and 7th July. Figure 53 shows a combination of a thermal image of the sample with a black and white, visible image of the target. It shows that the apparent surface temperature of the sample was varying by about 3 $^{\circ}$C over the measured area. The variation in temperature is due to a combination of true temperature changes due to the difference of the temperature of the sample and the air temperature as well as due to spatial emissivity variations on the surface of the sample.
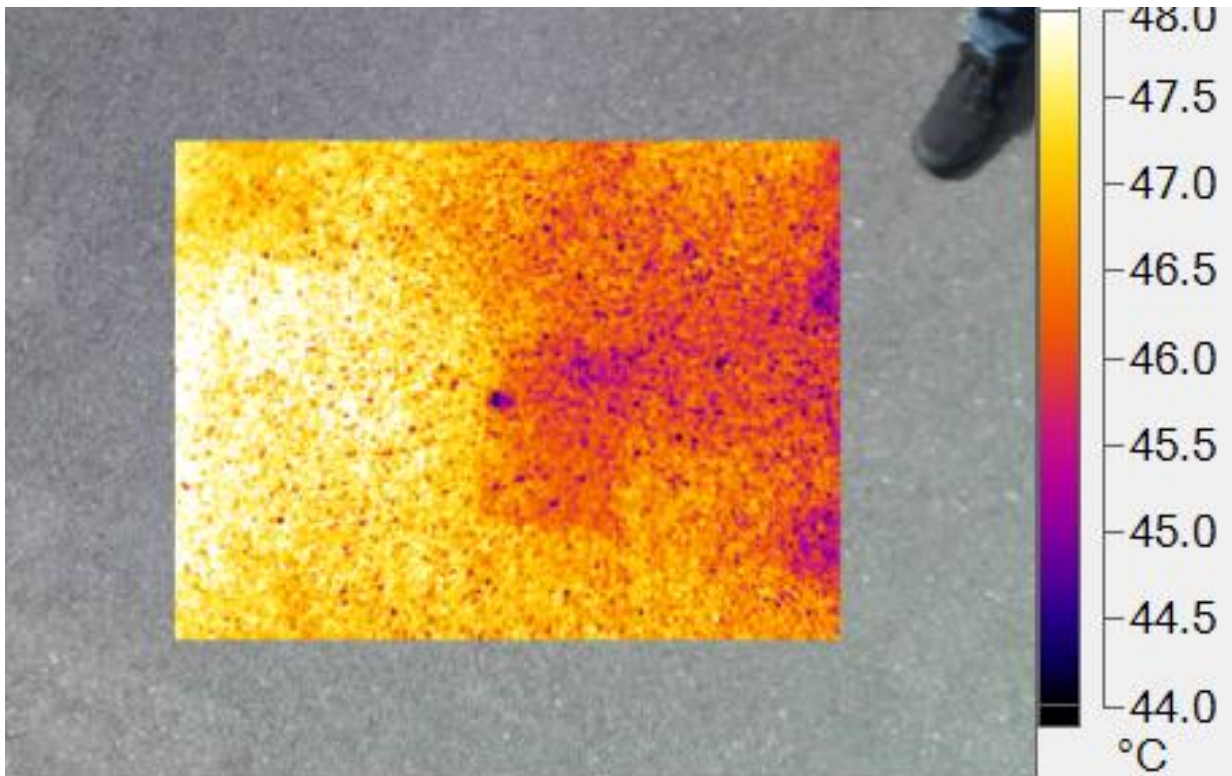

Figure 53: Combination of a thermal image of the asphalt/tarmac sample with a black and white, visible image of the same target. The Figure shows that the apparent surface temperature of the sample was varying by about 3 $^{\circ}$C over the measured area.

Figure 54 shows the measurements reported by the different participants on the 6th and 7th July. Figure 55 shows the difference between the measuring radiometers and their mean on the 6th and 7th July. Because participants provided their measurement at different times, a standard interpolation method was used to estimate the measurements of the different participants at 10 second intervals. The Figure 55 shows that the difference between all radiometers from their mean is largely within ± 2 $^{\circ}$C for both days during which measurements were done. Finally, Figure 56 shows the difference between the surface temperature of the tarmac/asphalt sample measured by participants and the mean of the measurements of all participants.
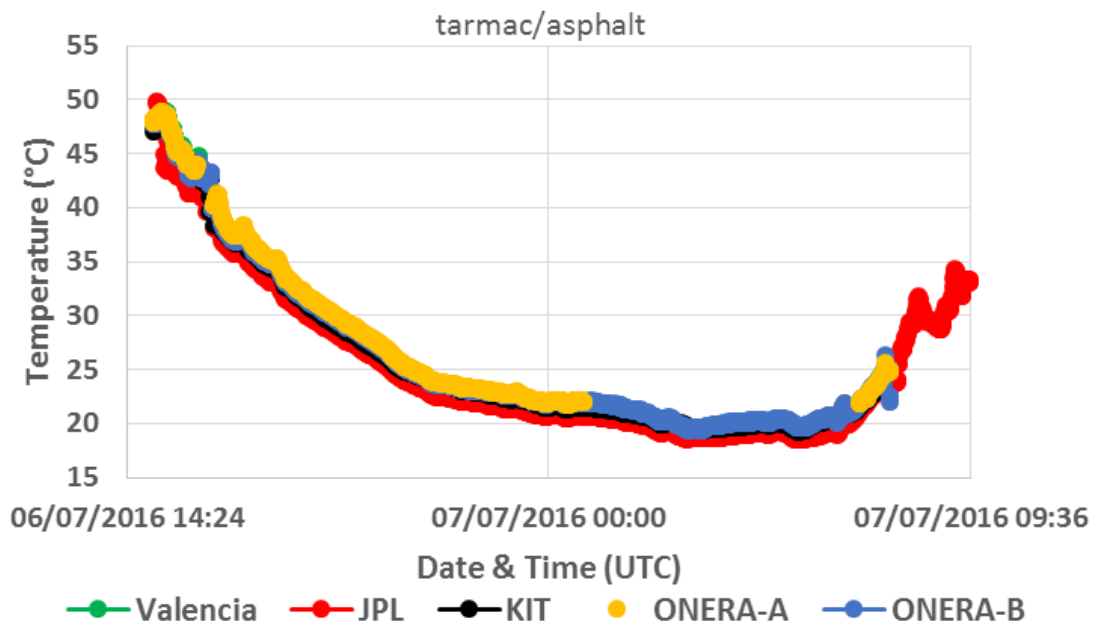
Figure 54: Surface temperature of tarmac/asphalt measured using the participating radiometers on the 6th and 7th July 2016.
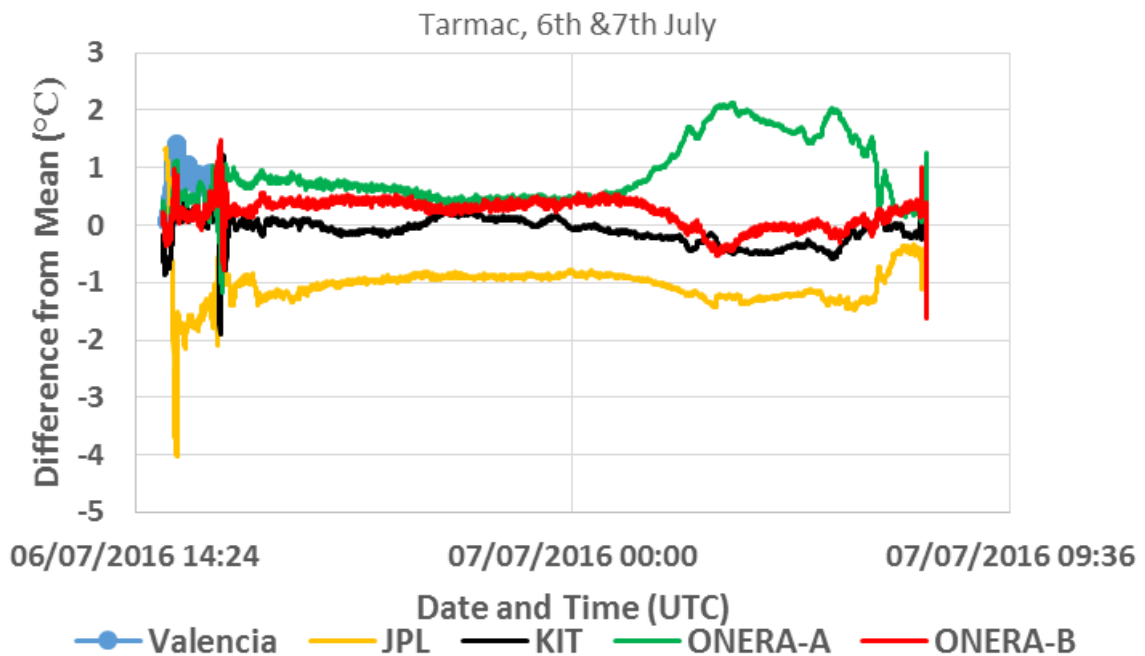

Figure 55: Difference between the measurements using each of the five measuring radiometers for the tarmac/asphalt sample and their mean. This Figure shows that the bulk of the measurements using all five radiometers agreed with their mean to within ±2 ºC throughout the monitoring period.
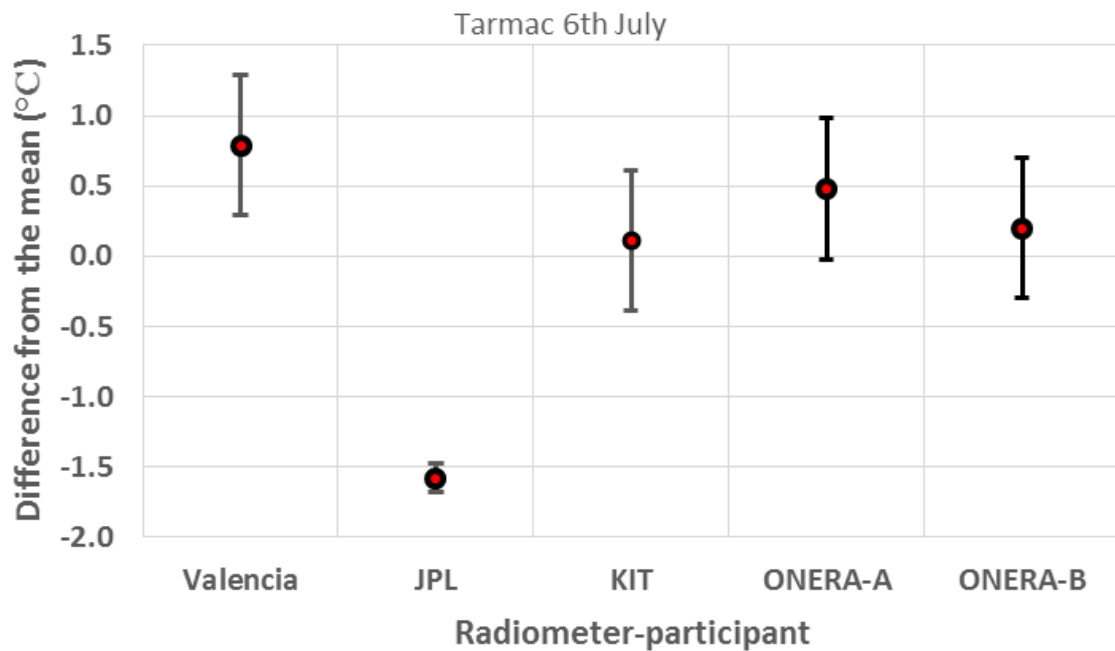
Figure 56: Difference between the surface temperature of the tarmac/asphalt sample measured by participants on 6th July and the mean of the measurements of all participants.

5. DISCUSSION

5.1 FIELD-OF-VIEW (FOV) ISSUES

The area of all samples was made large enough that it exceeded the area viewed by each of the participating radiometers and therefore the area viewed by the radiometers under-filled the area of the sample. However, the FoV of the radiometers was different so if all the radiometers were to be mounted at the same distance (height) from the target, the radiometers would be viewing different areas of the target. This was an issue to the comparison, if the samples exhibited spatial variations in their surface temperature. Examination of the surface temperature of the samples using a thermal imager showed that there were apparent temperature variations on the surfaces of all samples. However, while the spatial frequency of the temperature variations on some samples was relatively high compared to the FoV for all the radiometers (meaning that the temperature measurements using each of the radiometers should provide a good average of the surface temperature of the targets), the spatial frequency of variations on other samples was low (see for example Figure 46) meaning that measurements by different radiometers would depend on the area of the target on which was in their FoV. It was, therefore, decided to mount two radiometers with narrow FoV on a pole and maintain them at a distance of 4 m from the surface of the sample, so that the areas monitored by these radiometers were of comparable size to the areas measured by the other radiometers (all with larger FoV). Figure 57 shows a photo of the radiometers measuring the surface temperature of the sand sample, with one of the radiometers placed at a height of approximately 4 m.
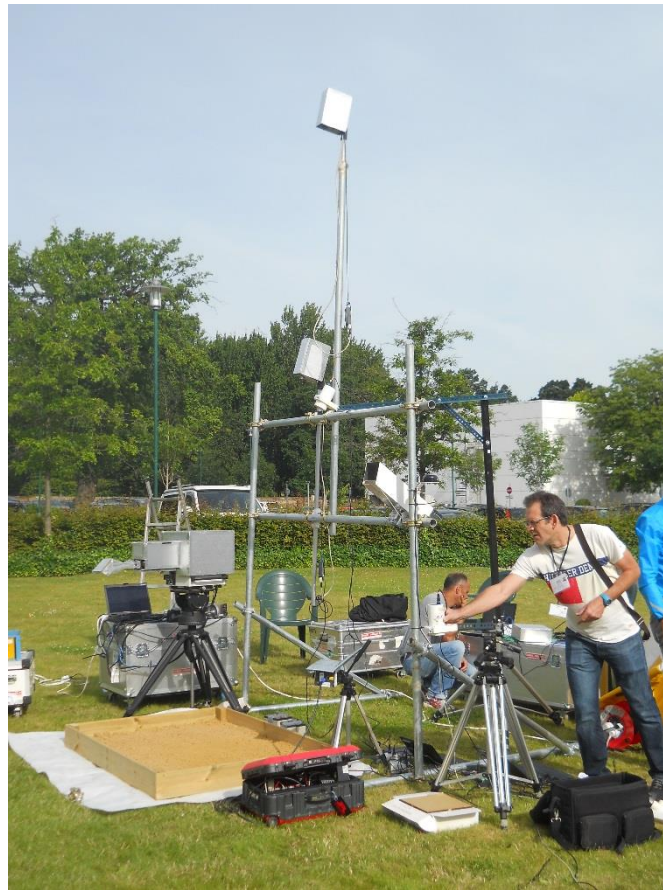
Figure 57: Radiometers measuring the surface temperature of the sand sample, with one of the radiometers placed at a height of approximately 4 m.

5.2 VARIATION IN THE SURFACE TEMPERATURE OF THE SAMPLES

Thermal images show that the surface temperature of all samples exhibits spatial temperature variations. These arise mainly from true temperature variations but also from variations in the emissivity of the samples. True temperature variations can arise from spatial variations of the properties of materials on the surface of the samples, e.g. thermal conductivity, emissivity, reflectivity, structure and small scale topography, surface roughness, etc. Peaks in the sample tended to have lower emissivities compared to troughs, where multiple reflections resulted in the radiation being trapped. Smoothing the surface of the samples was shown to reduce the apparent surface variations measured by the thermal imager. This was demonstrated very clearly on the sand sample which could be smoothed and made rough very easily. However, other samples such as the gravel sample could not be smoothed sufficiently due to the size of the particles. The sample which exhibited the smallest temperature variations was the tarmac/asphalt sample, partly because it had a relatively smooth surface and partly because it had relatively good thermal conductivity due to the binding of its constituents, which tend to even out any temperature non-uniformities.

5.3 EMISSIVITY OF THE SAMPLES

The determination of surface temperature of a sample depends critically on the knowledge of the emissivity of its surface. Three of the participants measured the emissivity of some of the samples during the measurement campaign. Valencia University measured the emissivity

values of all the samples (see Section 3.1.1 of this report) which also allowed them to estimate the uncertainty in the emissivity measurement. This uncertainty was then used to calculate the uncertainty contribution in the final surface temperature of the sample from the uncertainty in the measurement of the sample uncertainty (see Section 3.1.1 of this report).

KIT used the "box method" to measure the emissivity of four of the samples. KIT measured values of 0.9824 ± 0.0068, 0.9587 ± 0.0025, 0.952 ± 0.010 and 0.9592 ± 0.0053 for the emissivity of the soil, gravel, sand and tarmac samples respectively. However, due to adverse environmental conditions during some of the box measurements, the emissivity values for the clover and short grass were taken from literature instead. Values of 0.985 ± 0.005 and 0.98 ± 0.01 were used for the emissivity of clover and short grass samples. The full information on the emissivities used by KIT in association with their KT15.85 IIP radiometer can be found in Section 3.3.1.

ONERA estimated the emissivity of the target samples by sequentially measuring two radiance spectra using their BOMEM MR304SC FTIR spectroradiometer which was equipped with a 75 mrad FoV telescope and a 45° flat mirror. This method also required the use of a 10"x10" Labsphere Infragold reflector standard and their MIKRON M345 4"x4" blackbody set at two different temperatures (see Section 3.4.1 of this report).

Figure 58 shows the emissivity spectrum of the sand sample in the 800 cm^{-1} to 1250 cm^{-1} region, as measured by ONERA during the 2016 campaign. It is clear that the emissivity of this sample depends strongly on wavelength. Unfortunately, the spectral responsivity of the participating radiometers is different, and, indeed, their spectral responsivity peaks at different wavelengths. This means that there would be differences in the measurement of the surface temperature of a target even if the participants used the same emissivity value for that particular sample. Rather than insist that participants use the same emissivity value for a particular sample, it was considered far better to allow the participants to use what they consider as their best estimate of the target emissivity for their radiometer under the conditions which prevailed when the measurements were done. In fact this is the approach which they would have to use in the field during a measurement campaign. For this reason, no guidance was given as to which emissivity value participants should use for particular targets during the 2016 LST comparisons.

5.4 ATMOSPHERIC CONDITIONS

It should be pointed out that during the entire 2016 LST measurement campaign at NPL, atmospheric conditions were not ideal, with cloud cover changing very quickly during the measurements.
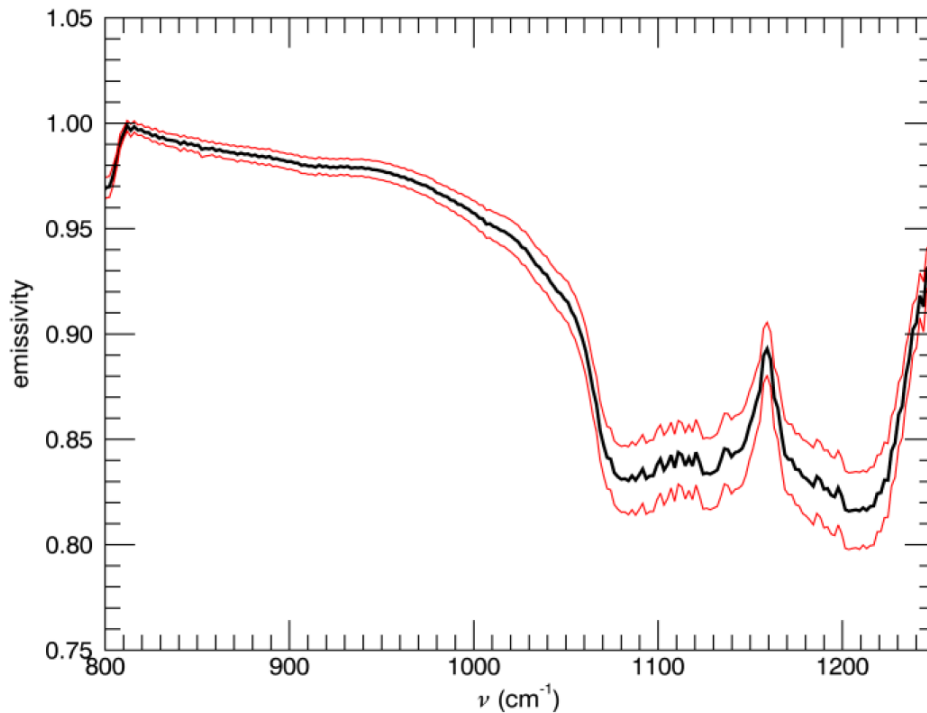
Figure 58: The emissivity of the sand sample in the 800 cm^{-1} to 1250 cm^{-1} region, as measured by ONERA during the 2016 FRM4STS comparison activity (data provided by ONERA).

5.5 LESSONS LEARNT.

The aim of this section is to highlight issues and lessons learnt during the 2016 LST radiometer comparison so that steps can be taken so their effects can be avoided or their effects diminished in future comparisons. A number of participants have contributed to the contents of this section.

    i.   The surface temperature of the target should be as homogeneous (spatially uniform) at least over the area of the target covered by the Field of View (FoV) of the participating radiometers.

    ii.   The area observed by the different radiometers should be large enough to average out possible surface temperature heterogeneities of the target within the radiometer FoV.

    iii.   Because different radiometers have different FoVs, it is recommended that in future comparisons, radiometers should be placed at different distances from the target being monitored so that the FoVs of the radiometers "cover" the same (identical) area of the target. The aim of this is to ensure that the same temperature non-uniformities at the surface of the target are seen (and averaged out) by every participating radiometer.

    iv.   Care should be taken to ensure that all participating radiometers are observing the same area of the target e.g. by employing a laser for their alignment.

    v.   LST determination should ideally be performed under clear sky conditions. Measurements performed under partly cloudy conditions should be avoided because

of the difficulties in estimating the corrections due to the sky radiance and temporal temperature fluctuations which a partly cloudy condition introduces.

vi. Ideally, each participant should measure the emissivity of the targets being measured and use these emissivity values in the calculation of their surface temperatures. This is the approach which was followed by a number of participants during the 2016 LST comparison. However, some participants sourced the emissivity values which they used from tables and published values. For this reason, it is recommended that in future comparisons, participants should also be provided with a common emissivity estimate which they should use to calculate another set of land surface temperatures of the targets. This will aid the identification of differences in the measurement techniques utilized by the different participants.

Acknowledgements

6. REFERENCES

Barker Snook, I., Theocharous, E. and Fox, N. P**.,** 2017, "2016 comparison of IR brightness temperature measurements in support of satellite validation. Part 2: Laboratory temperature comparison of radiation thermometers", NPL Report ENV 14, ISSN 2059-6030.

Barker Snook, I., Theocharous, E. and Fox, N. P., 2017a, "2016 comparison of IR brightness temperature measurements in support of satellite validation. Part 3: Water surface temperature comparison of radiation thermometers", NPL Report ENV 15, ISSN 2059-6030.

Barton, I. J., Minnett, P. J., Maillet K. A., Donlon, C. J., Hook, S. J., Jessup, A. T. and Nightingale, T.J., 2004, "The Miami 2001 infrared radiometer calibration and intercomparison: Part II Shipboard results", *Journal of Atmospheric and Oceanic Technology*, **21**, 268-283.

Rice, J. P., Butler, J. I., Johnson, B. C., Minnett, P. J., Maillet K. A., Nightingale, T. J, Hook, S. J., Abtahi, A., Donlon, and. Barton, I. J., 2004, "The Miami 2001 infrared radiometer calibration and intercomparison. Part I: Laboratory characterisation of blackbody targets", *Journal of Atmospheric and Oceanic Technology*, 21, 258-267.

Theocharous, E., Fox, N. P., Sapritsky, V. I., Mekhontsev, S. N. and Morozova, S. P., 1998, "Absolute measurements of black-body emitted radiance", *Metrologia*, **35**, 549-554.

Theocharous, E., Usadi, E. and Fox, N. P., 2010, **"**CEOS comparison of IR brightness temperature measurements in support of satellite validation. Part I: Laboratory and ocean surface temperature comparison of radiation thermometers", NPL Report COM OP3.

Theocharous, E. and Fox, N. P., 2010, "CEOS comparison of IR brightness temperature measurements in support of satellite validation. Part II: Laboratory comparison of the brightness temperature of blackbodies", NPL Report COM OP4.

Theocharous, E., Barker Snook, I. and Fox, N. P., 2017, "CEOS comparison of IR brightness temperature measurements in support of satellite validation. Part 1: Laboratory comparison of the brightness temperature of blackbodies", NPL Report ENV 12, ISSN 2059-6030.

Appendix A1: Images of the samples measured during the 2016 LST comparison at NPL

Figure A1-1: Photo of the short grass sample measured during the 2016 LST comparison at NPL

Figure A1-2: Photo of the clover sample measured during the 2016 LST comparison at NPL.
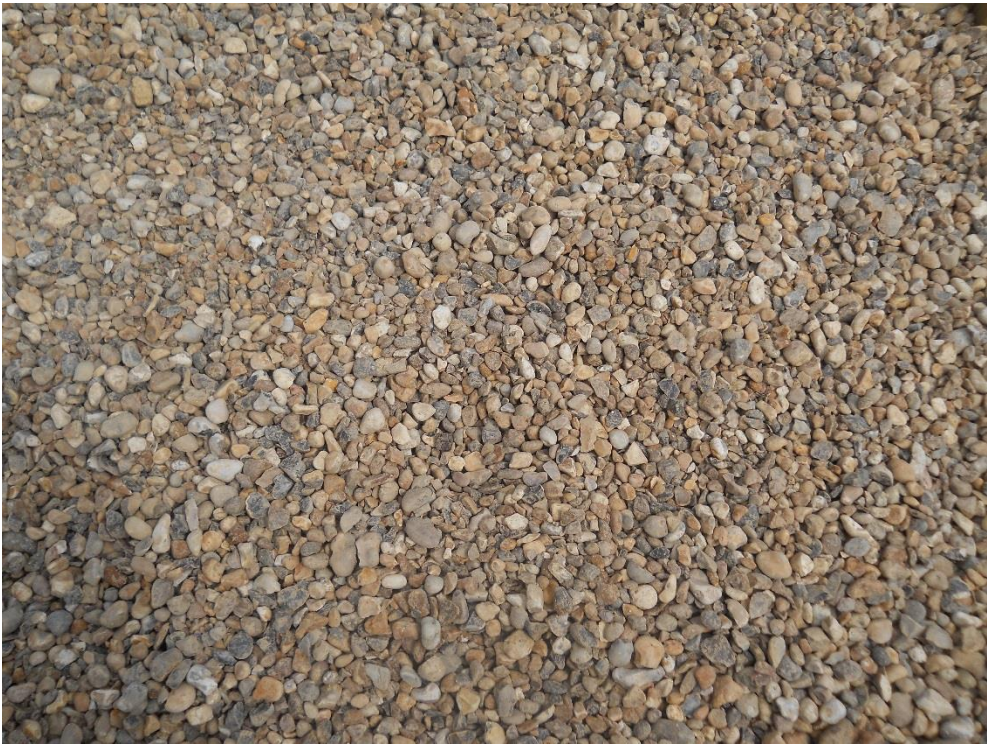
Figure A1-3: Photo of the short gravel sample measured during the 2016 LST comparison at NPL

Figure A1-4: Photo of the dark soil sample measured during the 2016 LST comparison at NPL.

Figure A1-5: Photo of the sand sample measured during the 2016 LST comparison at NPL

Figure A1-6: Photo of the asphalt/tarmac sample measured during the 2016 LST comparison at NPL